

1 **Multiple pathways of LRRK2-G2019S / Rab10 interaction in**
2 **dopaminergic neurons**

3 Alison Fellgett ¹, C. Adam Middleton ¹, Jack Munns ¹, Chris Ugboode ¹, David
4 Jaciuch ¹, Laurence Wilson ², Sangeeta Chawla ^{1,3} & Christopher J. H. Elliott ^{1,3}

5

6 1) Department of Biology, University of York, York, YO1 5DD, UK

7 2) Department of Physics, University of York, York, YO1 5DD, UK

8 3) York Biomedical Research Institute, Department of Biology, University of
9 York, YO1 5DD, UK

10 Correspondence to CJHE – Department of Biology, University of York, York,
11 YO1 5DD, UK. Email: cje2@york.ac.uk, Tel: +44 1904 328654

12

13 Jack Munns' present address : MRC Laboratory of Molecular Biology, Francis
14 Crick Avenue, Cambridge, CB2 0QH, UK

15 Keywords : *Drosophila*, dopamine, Leucine-rich-repeat-kinase2, bradykinesia,
16 vision, circadian rhythms, sleep, courtship memory.

17

18 Acknowledgements. We are grateful for the gifts of flies from Kristin Scott,
19 Wanli Smith, Cheng-Ting Chien, Julie Simpson, Serge Birman, and Stefan
20 Heidmann. We also thank the York Biology Technology Facility, Bloomington
21 Drosophila Supply Center and Flybase for their provision. Sean Sweeney,
22 Chris MacDonald and Amy Cording kindly read a draft manuscript. We are
23 particularly grateful to Parkinson's UK and to their volunteers for support (K-
24 1704, G-1804).
25

26 Abstract

27

28 **Background:** Inherited mutations in the LRRK2 protein are the most common
29 known cause of Parkinson's, but the mechanisms by which increased kinase
30 activity of mutant LRRK2 leads to pathological events remain to be
31 determined. *In vitro* assays (heterologous cell culture, phospho-protein mass
32 spectrometry) suggest that several Rab proteins might be directly
33 phosphorylated by *LRRK2-G2019S*. Which Rabs interact with LRRK2 in
34 dopaminergic neurons to facilitate normal and pathological physiological
35 responses remains to be determined. An *in vivo* screen of Rab expression in
36 dopaminergic neurons in young adult *Drosophila* demonstrated a strong
37 genetic interaction between *LRRK2-G2019S* and Rab10. We now ask if Rab10
38 is required for LRRK2-induced physiological responses in DA neurons.

39 **Methods:** *LRRK2-G2019S* was expressed in *Drosophila* dopaminergic neurons
40 and the effects of Rab10 depletion on Proboscis Extension, vision, circadian
41 activity pattern and courtship memory determined in aged flies.

42 **Results:** Rab10 loss-of-function rescued bradykinesia of the Proboscis
43 Extension Response (PER) and visual defects of aged flies expressing LRRK2-
44 G2019S in DA neurons. Rab10 knock-down however, did not rescue the
45 marked sleep phenotype which results from dopaminergic expression of
46 *LRRK2-G2019S*. Courtship memory is not affected by LRRK2 expression, but
47 is markedly improved by Rab10 depletion. Anatomically, both LRRK2-
48 G2019S and Rab10 are seen in the cytoplasm and at the synaptic endings of
49 dopaminergic neurons.

50 **Conclusions:** We conclude that, in *Drosophila* dopaminergic neurons, Rab10
51 is involved differentially in LRRK2-induced behavioral deficits. Therefore,
52 variations in Rab expression may contribute to susceptibility of different
53 dopaminergic nuclei to neurodegeneration seen in people with Parkinson's.

54

56 **Graphical Abstract**

57

58 Rab10 depletion ameliorates the proboscis extension bradykinesia and loss of

59 synaptic signalling in the retina induced by *LRRK2-G2019S* expression

60 (magenta arrows/orange crosses). Rab10 manipulation does not affect the

61 ‘sleep’ phenotype from *LRRK2-G2019S* (magenta arrow). Reduction of Rab10

62 facilitates conditioned courtship memory, but LRRK2 has no effect (yellow

63 arrow). All manipulations of Rab10 and *G2019S* in dopaminergic neurons,

64 shown in the outline of the brain (filled cells have high levels of Rab10). We

65 conclude that Rab10 and LRRK2 interact in some, but not all dopaminergic

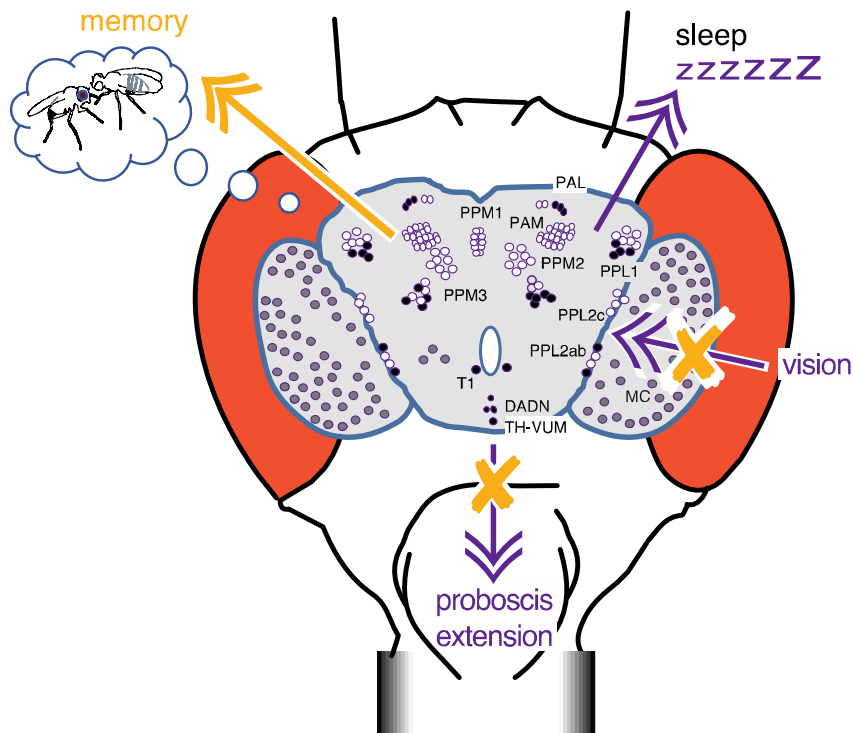
66 neurons. This may underlie differences in the susceptibility of different

67 human striatal dopaminergic cells to Parkinson’s and explain why different

68 symptoms initiate particular ages.

69

70



71

72

73 **Background**

74 Mutations in the *LRRK2* gene are the most frequent genetic cause of late onset
75 Parkinson's. The *G2019S* mutation increases LRRK2 kinase activity [1],
76 leading to a toxic cascade that kills dopaminergic neurons in the *substantia*
77 *nigra*. This results in bradykinesia and sleep disturbances, while loss of
78 dopaminergic amacrine cells in the retina contributes to visual deficits.
79 However, the main steps between LRRK2 and these pathological outcomes
80 remain to be determined. One of the first steps that has been suggested is that
81 LRRK2-G2019S may phosphorylate a number of small GTPases [3,5,8,10,29,35
82 & 43] [2]. Cell culture experiments have shown a particular effect on Rab10
83 [2–7], (see [8] for review), while a visual screen of *Drosophila* synaptic
84 processing indicated a particular synergy between Rab10 and G2019S [9]. As a
85 molecular switch, phosphorylation of a Rab protein could result in changed
86 effector binding with a series of downstream consequences. However, the
87 level of Rab10 is quite disparate, even among different types of dopaminergic
88 neurons [9,10] so that LRRK2 might not work in the same way in all
89 dopaminergic neurons.

90 Since most genetic mouse models of Parkinson's have very weak phenotypes,
91 with lack of neuropathology [11], we turned to the fly where manipulation of
92 Parkinson's disease related genes leads to marked phenotypes: bradykinesia
93 [12], loss of dopaminergic neurons [13], tremor [14], retinal degeneration [15]
94 and sleep disorder [16] (see, for review [17]). As in mammals, fly
95 dopaminergic neurons regulate movement, vision, sleep and memory.

96 To determine how important Rab10 is in the pathological cascade initiated by
97 LRRK2 activity, we now test the knock-down/knock-out of Rab10 in
98 dopaminergic neurons in the intact organism. We find the movement and
99 visual deficits seen in flies expressing *LRRK2-G2019S* in dopaminergic
100 neurons are rescued by the depletion of Rab10. However, the marked sleep
101 phenotype caused by dopaminergic expression of LRRK2-G2019S is not
102 affected by manipulation of Rab10. Conditioned courtship memory is not

103 affected by LRRK2, though dopaminergic Rab10 reduction markedly
104 improves this. We therefore find a role for Rab10 downstream of activated
105 LRRK2 in some, but not all, dopaminergic neurons in the activation of
106 LRRK2-associated physiological deficits in *Drosophila*.

107 **Materials and Methods**

108 **Flies:** All flies tested were male *Drosophila melanogaster*, using *TH-GAL4* (kind
109 gift of Serge Birman) to manipulate dopaminergic neurons or *nSyb-Gal4* (from
110 Julie Simpson (corresponding Bloomington stock 51635) for pan-neuronal
111 expression. *Gr5a-LexA* was used to express the LexOp-*ReachR*
112 channelrhodopsin in the sugar sensitive neurons independently from the
113 GAL4-UAS manipulations. Flies were raised and crossed using standard
114 *Drosophila* protocols [9]. The full list of fly lines is in Table 1.

115 **Validation of Rab10 knock-down and phosphorylation by G2019S:** We used
116 three strategies for Rab10 reduction. (i) We used a CRISPR/Cas9-generated
117 *Rab10* null [18], in which Rab10 was severely reduced (both pan-Rab10 and
118 phospho-Rab10 to less than 5% of wild-type, Fig. 1). This line was not used in
119 the visual assay because the retinal RFP marker causes the eyes to fluoresce
120 and this would distort the disco-chamber data. (ii) We used *Rab10^{RNAi}*. This
121 depleted phosphoRab10 (Fig. 1), but a small amount (~15%) of Rab10 was still
122 present (Fig. 1). (iii) We used the deGradFP technique to knockout *YFP-Rab10*
123 protein with the *vhhGFP* nanobody, to target *YFP-Rab10* to the proteasome.
124 This was used in flies in which the wild-type Rab10 had been replaced by
125 homologous recombination so that the *YFP-Rab10* was expressed at wild-type
126 levels. This reduced the amount of phospho-Rab10 to ~50% of wild-type (Fig.
127 1). In the *GFP-Rab10* background, expression of a RNAi against GFP depleted
128 some phospho-Rab10, but not as much as the nanobody, so we did not use
129 this further.

130 The ability of LRRK2-G2019S to phosphorylate Rab10 *in vivo* was confirmed
131 (Fig. 1Aiv; Biv), by comparing *nSyb > LRRK2-G2019S* with the kinase-dead
132 (KD) form (*LRRK2-G2019S-K1906M*). In the *nSyb > LRRK2-G2019S* flies, the

133 level of pRab10 was twice that of the controls, similar to the effect of pan-
134 neuronal expression of *Rab10*.

135 **Western Blots:** The levels of Rab10 and LRRK2-G2019S were assayed by
136 Western Blot using standard protocols [9,14]. For Rab10 the antibodies were:
137 α -pan-Rab10 (Nanotools, clone 605B11), α -phospho-Rab10 (Abcam, ab230261,
138 1:1000), and for LRRK2 (Neuromab, clone N241A/34). We used α -
139 synaptotagmin 91 as a loading control [19]. Selectivity of Rab10 antibodies
140 was confirmed by using a rat CNS extract [9]. For assay of *GFP-Rab10*, we
141 used Guinea pig anti-GFP (Synaptic Systems, 1:1000) as described recently [9].
142 Quantification of the blots was carried out in Fiji.

143 **Bradykinesia** was assessed using an optogenetic stimulus. Flies were fed
144 retinal (1 mM) pipetted onto the surface of their food for 1 week in the dark at
145 29 °C. They were restrained at 25 °C for 3 hours before the proboscis
146 extension responses were observed with a Grasshopper 3 (Point Grey) camera
147 mounted on a Zeiss Stemi microscope at 200 frames/second. A single flash
148 was delivered from a ThorM470L3 LED, driven at 8 V for 7 ms. The stimulus
149 was transcribed by *LexOp-ReachR* expressed in the Gr5a neurons. The area of
150 the video occupied by the proboscis was automatically analysed by python
151 code <https://github.com/biol75/PER>, and the Tukey - post-hoc test applied
152 in R.

153 **Akinesia** was recorded from 1 week old flies, kept in the dark at 29 °C. Flies
154 were restrained as described [14] and starved at 29 °C for 3 hours before being
155 offered a droplet of 100 mM sucrose three times. Each response was scored
156 Yes/No and the median response for each fly used. The χ^2 -post-hoc test
157 (Fifer) was done in R (3.3.3).

158 **Visual assays:** On the day of emergence, flies were placed in the dark or in
159 disco-chambers at 29 °C. 1 week old flies were prepared for SSVEP (Steady
160 State Visual Evoked Potential) measurements as recently described [9].
161 Stimuli were generated and responses recorded by an Arduino Due system
162 with FFTs and contrast sensitivity computed in Matlab. Dunnett's post-hoc

163 test was applied in R. Full code at <https://github.com/wadelab/flyCode>.
164 DPP (Deep-Pseudo-Pupil) images were captured with a Dino-Lite Camera
165 and software, and images cropped, quantified and converted to grey scale in
166 Fiji. Both images in Fig. 3Aii were combined in Fiji before the colour was
167 removed and the contrast increased.

168 **Circadian rhythms and sleep** patterns were recorded as described recently
169 [20] with a TriKinetics DAM system. Flies were placed in the monitor at 29 °C
170 on the day of eclosion, and locomotor activity was recorded in 1 minute bins
171 for 3 days under 12:12 h light/dark cycles followed by 7 to 10 days in constant
172 darkness. Activity data was analysed using the ActogramJ plugin for ImageJ
173 and sleep data using the ShinyR-DAM code [21] using the branch at
174 https://karolcichewicz.shinyapps.io/ShinyR-DAM_3_1_Beta/.

175 **Conditioned courtship memory** was recorded using the well-developed
176 conditioned courtship memory protocol for *Drosophila* [22,23]. One-week old
177 males, (kept at 29 °C), were provided with a virgin female and the time spent
178 in courting behaviours measured. Half of the males had recently (~ 30
179 minutes before) spent an hour with a mated female; half were naïve. Males
180 who fail to ‘remember’ their rejection will spend more time courting the
181 virgin female than controls. The Courtship Index (CI) was calculated as the
182 percentage of ten minutes that a male spent courting; and the memory index
183 (MI) by dividing the CI of each test fly by the mean CI of the naïve/sham flies
184 of the same genotype. A score of 0 indicates highest memory performance
185 possible and a score of ≥ 1 indicates no memory. The distribution of MI was
186 compared between genotypes using the Kolmogorov-Smirnov test. All naïve
187 and trained groups contained 16-23 flies.

188 **Immunocytochemistry** was performed on 3-5 day old flies expressing *G2019S*
189 as described recently [14], using the LRRK2 mouse antibody Neuromab (clone
190 N241A/34). In some flies, mCD8-GFP was also expressed in the
191 dopaminergic neurons. Each figure is representative of three preparations
192 from at least two crosses.

193

194 **Results**

195 To investigate a role for Rab10 in dopaminergic neurons, downstream of
196 activated LRRK2, we recombined the *Tyrosine-Hydroxylase* GAL4 with UAS-
197 *G2019S* and designated these ‘PD-mimic’ flies as *THG2*. We compared these
198 flies with controls in four types of behavioral/physiological phenotypes:
199 bradykinesia in the proboscis extension response, neural signalling in the
200 retina, sleep patterns and conditioned courtship memory. These four systems
201 are controlled by different clusters of dopaminergic neurons.

202 *Rab10* reduction rescues *LRRK2-G2019S* bradykinesia

203 The major features of Parkinson’s are movement deficits (bradykinesia),
204 slowing or loss of movement and tremor. We therefore begin our analysis
205 with the movement of PD-mimic *THG2* flies. The Proboscis Extension
206 Response (PER), a reaching movement used by Dipteran flies to obtain food,
207 is particularly amenable to analysis [24] (Fig. 2Ai). When a fly walks across a
208 surface and encounters a droplet of sugary solution, the sucrose-sensitive
209 neurons on the legs are stimulated and this elicits a rapid extension of the
210 proboscis. The PER is modulated by a single dopaminergic neuron, the
211 Tyrosine Hydroxylase Ventral Unpaired Median (TH-VUM) neuron [25],
212 which has a high level of Rab10 expression [9]. Expression of *G2019S* in this
213 neuron results in movement deficits – akinesia (loss of the PER), slower
214 response (bradykinesia) and tremor [14]. Further, the PER can be elicited
215 using an optogenetic stimulus. In this paradigm, the sucrose-sensitive sensory
216 neurons in the leg express a channelrhodopsin which is stimulated by a flash
217 of light. Expression of a channelrhodopsin by the LexA/LexOp system in the
218 sugar-sensitive ‘Gr5a’ neurons on the leg is independent of the expression of
219 *LRRK2-G2019S* in the TH-VUM and other dopaminergic neurons by the
220 GAL4-UAS system [26]. This precise control of the stimulus makes it possible
221 to measure the time course of the reaching movement, and separates the

222 activation of the stimulus from manipulations using the GAL4 system in the
223 dopaminergic neurons.

224 In our optogenetic setup, 60% of control flies respond to a single flash of light
225 by smoothly extending their proboscis, whereas flies in which *Tyrosine-*
226 *Hydroxylase* GAL4 was used to express *LRRK2-G2019S* (*THG2*) only respond
227 30% of the time, i.e. *G2019S* induces akinesia (Fig. 2Aii). Those *THG2* flies that
228 do respond, take ~100 ms longer to achieve maximum extension, showing
229 bradykinesia (Fig. 2Aiii, iv). Knock-down of Rab10 using *Rab10^{RNAi}* co-
230 expressed with *LRRK2-G2019S* in the dopaminergic neurons, fully reverts
231 both akinesia and the bradykinesia (Fig. 2Aii-iv).

232 We next tested if Rab10 knock-down would also rescue the deficits induced
233 by *G2019S* in response to the natural stimulus, a sugar solution. Just over two-
234 thirds of control flies respond to sucrose (70%, Fig. 2Bi, green bars), whereas
235 less than half of *THG2* flies respond to sucrose (46 %, Fig. 2Bi, magenta). This
236 deficit is fully rescued when *Rab10^{RNAi}* is co-expressed with *THG2* (*THG2* >
237 *Rab10^{RNAi}* Fig. 2Bi, yellow). Dopaminergic expression of *Rab10^{RNAi}* alone has
238 no effect on the proportion of flies that respond to the sucrose solution (*TH* >
239 *Rab10^{RNAi}*, Fig. 2Bi, green).

240 As RNAi may have off-target effects, we supplemented this with a nanobody-
241 mediated-protein knockdown technique, deGradFP [27,28]. In this, we
242 deployed flies in which the wild-type *Rab10* gene had been replaced by *YFP-*
243 *Rab10* by homologous recombination. Then we expressed an anti-GFP
244 nanobody (*vhhGFP*) to deplete YFP-Rab10 protein in just the dopaminergic
245 neurons using *TH-GAL4*. In this experiment, *YFP-Rab10* flies with both
246 *G2019S* and *vhhGFP* expression (Fig. 2Bii, yellow bar) responded identically to
247 wild-types, or *YFP-Rab10* controls in which dopaminergic neurons expressed
248 just *vhhGFP* (Fig. 2Bii, *YFP-Rab10; TH* > *vhhGFP* green bar). This indicates a
249 full rescue of the *THG2* induced akinesia. We confirmed that expressing
250 *G2019S* and *vhhGFP* in flies with wild-type *Rab10* still resulted in akinesia
251 (Fig. 2Bii, magenta bar).

252 While the *Rab10* knockout is lethal in mammals [29], the fly *Rab10* null
253 (*Rab10⁻*) is viable [18]. We therefore tested if a global removal of Rab10 would
254 also ameliorate the akinesia deficit in the *THG2* flies. In the *Rab10⁻*
255 background, the *THG2* Proboscis Extension Response is fully rescued (Fig.
256 2Biii, orange), to the same level as wild-type controls (Fig. 2Bi, green). In
257 control experiments, the proportion of *Rab10⁻* flies that responded to sucrose
258 was identical to wild-types; this was true for the homozygote stock and for an
259 outcross to *TH* in males (*Rab10* is on the X-chromosome)(Fig. 2Biii, pale
260 green).

261 Rab10 is known to be phosphorylated by LRRK2 *in vitro* [2] and in the fly, *in*
262 *vivo* (Fig. 1). Phosphorylation is likely to be part of the activation mechanisms
263 of Rab10. If increasing phosphorylation of Rab10 is a key event in *LRRK2-*
264 *G2019S* driven dysfunction in dopaminergic neurons, we would expect
265 dopaminergic expression of *Rab10* to phenocopy that of *G2019S*. We found
266 that 55% of such *TH > Rab10* flies responded to sucrose, in an almost identical
267 manner to the *THG2* flies (Fig. 2Biv) with pronounced akinesia. No further
268 increase in akinesia is seen when both *G2019S* and *Rab10* are expressed at the
269 same time.

270 To confirm that akinesia was solely dependent on dopaminergic Rab10, we
271 took the *Rab10* null, and crossed it with flies expressing Rab10 in just the
272 dopaminergic neurons. Such *Rab10⁻; TH > Rab10* flies have akinesia when
273 compared with the *Rab10⁻* flies (Fig. 2Biii). Similarly, the *Rab10⁻; THG2 >*
274 *Rab10* show less response than *THG2 > Rab10* flies.

275 Thus, the *G2019S*-induced movement deficits in the PER are rescued by
276 depleting Rab10 in the dopamine neurons either at the mRNA level using
277 RNAi, or at the protein level using a nanobody, or with the global null.
278 Increasing Rab10 in the dopaminergic neurons induces akinesia similar to the
279 expression of *LRRK2-G2019S*.

280 *Dopaminergic reduction in Rab10 rescues G2019S-induced visual deficits*

281 People with Parkinson's also show visual deficits including loss of
282 dopaminergic neurons from the retina [30,31]. Aged *THG2* flies also show
283 strong retinal degeneration with vacuoles throughout the optic lobe [15]. To
284 demonstrate retinal degeneration, we deployed the 'Deep-Pseudo-Pupil'
285 (DPP) assay [32]. When wild-type flies are illuminated from below, they
286 show a DPP, with about 6-8 glowing ommatidia. In this, the normal retinal
287 structure focuses light from directly below towards the observer through the
288 center of the ommatidium, whereas light which is off-center is blocked by the
289 pigment granules at the edge of the ommatidium (Fig. 3Ai). We tested several
290 types of genetic background for the *THG2* 'PD—mimic' flies used in
291 movement assays and found that the contrast between DPP and the red eye
292 pigment was best when the *THG2* was in the deGradFP background.
293 Although the DPP was clear in these young flies, in flies aged for 14 days, the
294 DPP is distorted in these *THG2;vhhGFP* flies (Fig. 3A ii-iv). The outline of the
295 DPP is irregular, rather than a neat ellipse, and the number and dispersion of
296 the glowing ommatidia was increased. However, when dopaminergic *Rab10*
297 is depleted in the *THG2* deGradFP fly, the DPP is much less disrupted (*YFP-*
298 *Rab10; THG2 > vhhGFP* Fig. 3A ii-iv). There are fewer light-transmitting
299 ommatidia and they are all adjacent. Thus, dopaminergic *Rab10* reduction is
300 sufficient to rescue the *G2019S*-induced neurodegeneration. We conclude that
301 expression of *G2019S* leads to degeneration of the retina, including a
302 lysosomal deficit in the pigment granules.

303 In People with Parkinson's, the retinal degeneration of dopaminergic
304 amacrine cells is accompanied by changes in contrast detection e.g. [33]. We
305 therefore tested if the anatomical degeneration of the fly eye is linked to a loss
306 of visual physiological contrast sensitivity. To do this, we used the SSVEP
307 (Steady State Visual Evoked Potential) method which is automated to
308 distinguish the photoreceptor contrast sensitivity from the synaptic response
309 of the second order lamina neurons. At 7 days, all dark-reared control and
310 *THG2* flies show a strong SSVEP photoreceptor signal, indicating that the eyes
311 are functioning normally. There is no effect of the manipulation of *Rab10* (Fig.

312 3B, solid bars). On the other hand, when exposed to a mild visual stress to
313 accelerate neurodegeneration (by being kept in the disco chamber for 1 week
314 [15]), the *THG2* flies lose almost all their visual response – it is reduced to
315 18 % of the wild-type dark level (Fig. 2Bii,iii, hatched magenta bars; controls
316 in green), indicating loss of photoreceptor function. As with the anatomical
317 measure, the contrast sensitivity of the eye was rescued using the deGradFP
318 manipulation (*YFP-Rab10; THG2 > vhhGFP*, Fig. 2Bi, yellow bar). With co-
319 expression of *Rab10^{RNAi}*, this *THG2* deficit is also fully rescued (Fig. 3Dii,
320 yellow bar).

321 Thus, both electrophysiological response and structural observation of the
322 DPP indicate that *Rab10* knock-down rescues the effect of dopaminergic
323 *LRRK2-G2019S*.

324 *LRRK2-induced daily activity deficits are not affected by Rab10*

325 A third behavior modulated by dopaminergic neurons is the daily sleep-wake
326 rhythm, both in human [34] and fly [35] (see [36] for review). The
327 dopaminergic neurons in the fly mushroom bodies are key players in the
328 daily activity rhythm. Locomotor activity during light/dark cycles provides a
329 measure of circadian rhythm and sleep-wake behavior (Fig. 4A). Periods of
330 inactivity longer than 5 minutes defined as ‘sleep’ (see [37]). In 12h:12h light
331 on:off cycles, all flies tested show a daily sleep-wake rhythm, sleeping more in
332 the light than in the dark, with *THG2* flies sleeping ~15% more than the
333 controls during the ‘day’ (Fig. 4B). At the light/dark transition, all flies have
334 high, persistent activity, and little sleep. *THG2* flies continue their activity
335 during the dark, spending less than 50% of the time ‘asleep’ in the dark that
336 control flies managed (*TH/+*, Fig. 4B). Neither reduction nor increased
337 expression of *Rab10* in dopaminergic neurons affected the sleep/wake cycle
338 of either the control or *LRRK2-G2019S* flies. Following light-dark entrainment
339 (LD), in the dark (DD), the fly locomotor activity pattern persists with a ~24
340 hour cycle providing a measure of intrinsic circadian rhythms. The period of
341 the circadian rhythm was not affected by *LRRK2-G2019S* or *Rab10*

342 manipulation, though a small reduction was seen when both transgenes were
343 expressed (Fig. 4A). This is not unexpected as the circadian period is not
344 affected by dopamine manipulations [38].

345 Thus, the normal sleep-wake cycle is disrupted by dopaminergic *LRRK2-*
346 *G2019S*, but not by *Rab10* manipulation, even though Rab10 in the context of
347 LRRK2-G2019S is seen to regulate the Proboscis Extension Response and
348 retina.

349 *Improved Memory-due to Rab10 depletion are insensitive to LRRK2-G2019S*

350 Dopaminergic circuits also affect memory in both human [39] and fly [40,41].
351 We deployed the conditioned courtship short-term memory protocol, which
352 is dependent on the well-known dopaminergic MB neurons [42] to assess the
353 effects of Rab10 and *G2019S*. In this assay, males are allowed to court mated
354 females, which reject their advances. When presented with more receptive
355 virgin females, they tend to court less as they ‘remember’ their rejection. We
356 found that dopaminergic knock-down of Rab10 substantially reduced the
357 memory index, with over half of the *TH > Rab10^{RNAi}* flies having a memory
358 index less than 0.05, i.e. they have excellent memory. In contrast, only 10% of
359 control flies had a memory index less than 0.05 (Fig. 5A). When *G2019S* was
360 expressed, no change in the distributions was seen, and Rab10 depletion still
361 improved memory (Fig. 5B).

362 We conclude that, in the conditioned courtship assay, Rab10 is present and
363 has a key role in the dopaminergic neurons, but that the behavior is not
364 affected by dopaminergic expression of *G2019S*.

365 *Cytoplasmic Location of G2019S and Rab10*

366 In *THG2* flies, ectopically expressed LRRK2-G2019S protein is detected in
367 dopaminergic neurons more strongly in the cytoplasm than the nucleus (Fig.
368 6A). The highest expression intensity is seen in the cytoplasm surrounding the
369 nucleus and is quite uneven, with small holes, possibly representing the
370 absence of the LRRK2 protein from lysosomes or mitochondria. Additionally,

371 there is very weak staining along the axons and of the synaptic endings,
372 including the mushroom bodies and fan-shaped body (Fig. 6C). A similar
373 pattern of staining is seen with dopaminergic expression of *hLRRK2-wild-type*
374 (data not shown). Rab 10 expression (*TH > Rab10-YFP* flies, Fig. 6B) shows a
375 staining in the cytoplasm, with the strongest fluorescence at the synaptic
376 terminals, noticeably in the neuropil of the mushroom bodies and fan-shaped
377 body.

378 Discussion

379 Having previously demonstrated a strong genetic interaction, *in vivo*, between
380 LRRK2 and Rab10 [9], we sought to determine whether manipulation of
381 Rab10 affected the physiological deficits associated with flies expressing
382 LRRK2 G2019S. We have identified a requirement for Rab10 in mediating the
383 movement and visual deficits induced by dopaminergic expression of *LRRK2-*
384 *G2019S*. In contrast, in two other dopaminergic physiological systems, there
385 was no interaction: in one (the circadian sleep/wake cycle) *LRRK2-G2019S*
386 has a marked phenotype independent of Rab10; in the other (conditioned
387 courtship memory) Rab10 has a distinct role, but there is no *LRRK2-G2019S*
388 phenotype. As such, we have begun to identify the individual dopaminergic
389 circuits in the fly that are most sensitive to LRRK2-Rab10 interplay.

390 *Rab10 knock-down rescues movement and visual deficits from dopaminergic LRRK2-* 391 *G2019S expression*

392 Movement and visual deficits induced by LRRK2-G2019S expression have
393 been linked to low dopamine release in the TH-VUM and some PPL/MC
394 neurons that control the PER and vision respectively [14,15]. We focus here on
395 how the LRRK2-Rab10 interaction might lead to a potential loss of dopamine
396 release. First, *Rab10* is strongly expressed in these neurons [9] and so could
397 play a role in controlling dopamine traffic or exocytosis. *LRRK2-G2019S*
398 expression in the fly CNS increases the phosphorylation of Rab10
399 approximately two-fold. Knock-down by *Rab10^{RNAi}* reduces the level of
400 pRab10 below the level at which it is detected, though some Rab10 is still

401 present. Additionally, protein knock-down using deGradFP lowers pRab10
402 and rescues the proboscis extension/visual deficits, though the reduction in
403 Rab10 reported by Western Blot was not so strong as with *Rab10^{RNAi}*. Thus,
404 the amelioration, *in vivo* of *G2019S*-induced movement and visual deficits by
405 *Rab10^{RNAi}* is in accord with data from cell culture that Rab10 is a key target of
406 LRRK2 [2–7]. Our data additionally shows, at least for a subset of *Drosophila*
407 dopaminergic neurons, Rab10 is likely the relevant physiological substrate for
408 LRRK2-*G2019S*.

409 This genetic interaction between Rab10 and LRRK2-*G2019S* does not imply
410 that the physical interaction is direct, though the anatomical evidence shows
411 that both proteins spread along the axons to the synaptic endings and are
412 likely in proximity. Rab proteins often work in functionally linked chains e.g.
413 [43,44]. Our data does not exclude that the *LRRK2-G2019S* deficits also
414 involve other Rabs.

415 The cellular consequences of phosphorylation of Rab10 are not yet fully clear,
416 but it has been suggested that this may switch the effectors to which Rab10
417 binds [8,44,45]. In dividing cells in culture phosphorylation of Rab10 by
418 LRRK2 reduces ciliogenesis [46,47]. However, the relevance of this to the
419 terminally differentiated adult *Drosophila* CNS neurons is not clear. Both
420 LRRK2 and Rab10 have been linked to mitochondrial damage resolution,
421 through the Rab10 effector OPTN (optineurin) [48] though *Drosophila* do not
422 have an evident OPTN homolog (this function could be fulfilled by an as yet
423 unidentified protein). Another role for LRRK2 – control of vesicle transport at
424 the TGN – has support from HEK cells [49] and fly neurons. In the fly retina,
425 a Rab10 interaction has been reported occurring at the TGN with its GEF Crag
426 and effector Ehbp1 [50], affecting vesicle budding. Interestingly, the fly
427 ortholog of LRRK2, which is dLRRK, is linked to the golgin protein, Lava
428 lamp, at Golgi outposts in neurites [51]. An effect on vesicle transport at the
429 TGN, along with consequent endosomal disruption [43,52–54] may provide
430 an explanation for a lack of dopamine release.

431 *Sleep/wake cycles and conditioned courtship memory do not depend on an interaction*
432 *between Rab10 and LRRK2-G2019S*

433 In stark contrast, in the same animals, dysfunction in other dopamine-
434 mediated behaviours does not require Rab10. *Rab10^{RNAi}* did not ameliorate the
435 change in daily sleep defect induced by LRRK2-G2019S, and overexpression
436 of Rab10 did not phenocopy G2019S- induced sleep defects. While *Rab10^{RNAi}*
437 expression affected the conditioned courtship memory, indicating the
438 presence of Rab10 and its importance in these dopaminergic neurons, *LRRK2-*
439 *G2019S* had no phenotype. Thus, Rab10 seems to be present, but not affected
440 by *LRRK2-G2019S*.

441 Dopaminergic neurons display varied levels of Rab10 even within a
442 particular cluster [9]. Consequently, it is possible that the Rab10 GEFs, GAPs
443 and effectors may also differ between the subsets of the dopaminergic
444 neurons in the PAM, PPL1 and PPM3 neurons, the clusters that regulate the
445 sleep-wake cycle [35,55,56]. The pattern of gene expression in the three types
446 of PAM neurons is complex [10]. The GEF *Crag* was expressed in only one
447 type; the GAPs *Evi5* and *plx* in different types, while the effector pattern is
448 more complex: *Ehbp1* and *Rilpl (CG11448)* in all three PAM-types but another
449 effector (*Mical*) is present in none. This suggests that Rab10 function may be
450 regulated differentially in different dopaminergic neuronal clusters. Further,
451 *dLRRK* is expressed in the dopaminergic neurons in to optic lobe, but not in
452 the PAM neurons [10]. The variation in gene expression may explain why
453 some labs have identified other potential LRRK2 interactors – for example
454 EndophilinA, in *Drosophila* larval glutamatergic neuromuscular synapses
455 [57].

456 **Conclusion:** Our key finding is that that LRRK2-G2019S may signal by
457 several pathways, even within the dopaminergic neuron population. We
458 conclude that an uneven distribution of Rabs, their effectors and binding
459 partners may contribute to the differences in the rate of dopaminergic neuron

460 degeneration in the human striatum. Multiple LRRK2 pathways may also
461 explain why the range of Parkinson's symptoms initiate at different ages.

462

463

464

465

466 Table of Abbreviations

Abbreviation	Full text
CI	Courtship Index
DAM	Drosophila activity monitor
dLRRK	The Drosophila homolog of LRRK2
DPP	Deep-Pseudo-Pupil
FFT	Fast-Fourier Transform
Gal4/UAS	A binary system for targeted gene expression in the fly
GAP	GTPase-activating protein
GEF	Guanine nucleotide exchange factor
LED	Light-Emitting Diode
LexA/LexOp	A second, independent binary system for targeted gene expression in the fly
LRRK2	Leucine-rich-repeat kinase2
MC	dopaminergic neurons in the optic lobe (also known as Mi15 neurons)
MI	Memory index
nSyb	neuronal Synaptobrevin
OPTN	optineurin
PAM	A cluster of dopaminergic neurons in the fly brain
PER	Proboscis Extension Response
PPL	A second cluster of dopaminergic neurons in the fly brain
PPM	Another cluster of dopaminergic neurons in the fly brain
SSVEP	Steady State Visual Evoked Potential
TGN	Trans-Golgi Network
TH	Tyrosine-Hydroxylase
TH-VUM	Tyrosine Hydroxylase Ventral Unpaired Median neuron
<i>THG2</i>	Flies with TH Gal4 recombined with UAS-LRRK2-G2019S (PD-mimic)
YFP	Yellow Fluorescent Protein

467

468 **Declarations**

469 Ethics approval and consent to participate. All experiments are with

470 *Drosophila melanogaster* and do not require consent.

471 Consent for publication. All authors read and approved the final manuscript.

472 Availability of data and material. Full statistical and genetic data is available

473 in the Supplementary Tables, and the raw data is available on request

474 Competing interests. None declared

475 Funding: Parkinson's UK, (K-1704, G-1804).

476 Authors' contributions AF, CAM, JM, CU, DJ performed experiments, SC and

477 LW developed apparatus/methods, SC and CJHE analysed data, CJHE

478 drafted the manuscript, which was edited by SC, JM, DJ and CJHE.

479

480

481 REFERENCES

482

- 483 1. Greggio E, Cookson MR. Leucine-Rich Repeat Kinase 2 Mutations and
484 Parkinson's Disease: Three Questions. *ASN Neuro*. 2009;1:AN20090007.
- 485 2. Steger M, Diez F, Dhekne HS, Lis P, Nirujogi RS, Karayel O, et al.
486 Systematic proteomic analysis of LRRK2-mediated Rab GTPase
487 phosphorylation establishes a connection to ciliogenesis. *Elife*. 2017;6:e31012.
- 488 3. Fan Y, Howden AJM, Sarhan AR, Lis P, Ito G, Martinez TN, et al.
489 Interrogating Parkinson's disease LRRK2 kinase pathway activity by
490 assessing Rab10 phosphorylation in human neutrophils. *Biochem J*.
491 2018;475:23–44.
- 492 4. Jeong GR, Jang E-H, Bae JR, Jun S, Kang HC, Park C-H, et al. Dysregulated
493 phosphorylation of Rab GTPases by LRRK2 induces neurodegeneration. *Mol*
494 *Neurodegener*. 2018;13:8.
- 495 5. Thirstrup K, Dächsel JC, Oppermann FS, Williamson DS, Smith GP, Fog K,
496 et al. Selective LRRK2 kinase inhibition reduces phosphorylation of
497 endogenous Rab10 and Rab12 in human peripheral mononuclear blood cells.
498 *Sci Rep*. 2017;7:10300.
- 499 6. Liu Z, Bryant N, Kumaran R, Beilina A, Abeliovich A, Cookson MR, et al.
500 LRRK2 phosphorylates membrane-bound Rabs and is activated by GTP-
501 bound Rab7L1 to promote recruitment to the trans-Golgi network. *Hum Mol*
502 *Genet*. 2018;27:385–95.
- 503 7. Kelly K, Wang S, Boddu R, Liu Z, Moukha-Chafiq O, Augelli-Szafran C, et
504 al. The G2019S mutation in LRRK2 imparts resiliency to kinase inhibition. *Exp*
505 *Neurol*. 2018;309:1–13.
- 506 8. Alessi DR, Sammler E. LRRK2 kinase in Parkinson's disease. *Science (80-)*.
507 2018;360:36–7.
- 508 9. Petridi S, Middleton CA, Ugbo C, Fellgett A, Covill L, Elliott CJH. In

- 509 Vivo Visual Screen for Dopaminergic Rab ↔ LRRK2-G2019S Interactions in
510 *Drosophila* Discriminates Rab10 from Rab3. *G3 (Bethesda)*. 2020;10:1903–14.
- 511 10. Davis FP, Nern A, Picard S, Reiser MB, Rubin GM, Eddy SR, et al. A
512 genetic, genomic, and computational resource for exploring neural circuit
513 function. *Elife*. 2020;9:1–40.
- 514 11. Daniel G, Moore DJ. Modeling LRRK2 pathobiology in Parkinson’s
515 disease: From yeast to rodents. *Curr Top Behav Neurosci*. 2014;22:331–68.
- 516 12. Feany MB, Bender WW. A *Drosophila* model of Parkinson’s disease.
517 *Nature*. 2000;404:394–8.
- 518 13. Liu Z, Wang X, Yu Y, Li X, Wang T, Jiang H, et al. A *Drosophila* model for
519 LRRK2-linked parkinsonism. *Proc Natl Acad Sci U S A*. 2008;105:2693–8.
- 520 14. Cording AC, Shiaelis N, Petridi S, Middleton CA, Wilson LG, Elliott CJH.
521 Targeted kinase inhibition relieves slowness and tremor in a *Drosophila*
522 model of LRRK2 Parkinson’s. *npj Park Dis*. 2017;3:34.
- 523 15. Hindle SJ, Afsari F, Stark M, Middleton CA, Evans GJO, Sweeney ST, et al.
524 Dopaminergic expression of the Parkinsonian gene LRRK2-G2019S leads to
525 non-autonomous visual neurodegeneration, accelerated by increased neural
526 demands for energy. *Hum Mol Genet*. 2013;22:2129–40.
- 527 16. Julienne H, Buhl E, Leslie DS, Hodge JLL. *Drosophila* PINK1 and parkin
528 loss-of-function mutants display a range of non-motor Parkinson’s disease
529 phenotypes. *Neurobiol Dis*. 2017;104:15–23.
- 530 17. Hewitt VL, Whitworth AJ. Mechanisms of Parkinson’s Disease. *Curr Top*
531 *Dev Biol*. 2017. p. 173–200.
- 532 18. Kohrs FE, Daumann I, Pavlović B, Jin EJ, Lin S-C, Port F, et al. Systematic
533 functional analysis of Rab GTPases reveals limits of neuronal robustness in
534 *Drosophila*. *bioRxiv*. 2020;2020.02.21.959452.
- 535 19. West RJH, Lu Y, Marie B, Gao F-B, Sweeney ST. Mutations in Rab8
536 Identify A POSH/TAK1 Signal Regulating Synaptic Growth in *Drosophila*. *J*

- 537 cell biol. 2015;in press.
- 538 20. Nippe OM, Wade AR, Elliott CJH, Chawla S. Circadian Rhythms in Visual
539 Responsiveness in the Behaviorally Arrhythmic *Drosophila* Clock Mutant *Clk*
540 *Jrk*. *J Biol Rhythms*. 2017;32:583–92.
- 541 21. Cichewicz K, Hirsh J. ShinyR-DAM: a program analyzing *Drosophila*
542 activity, sleep and circadian rhythms. *Commun Biol*. 2018;1:25.
- 543 22. Griffith LC, Ejima A. Courtship learning in *Drosophila melanogaster*:
544 Diverse plasticity of a reproductive behavior. *Learn Mem*. 2009;16:743–50.
- 545 23. Koemans TS, Oppitz C, Donders RAT, van Bokhoven H, Schenck A,
546 Keleman K, et al. *Drosophila* Courtship Conditioning As a Measure of
547 Learning and Memory. *J Vis Exp*. 2017;e55808.
- 548 24. Dethier VG. The hungry fly: A physiological study of the behavior
549 associated with feeding. 1976.
- 550 25. Marella S, Mann K, Scott K. Dopaminergic modulation of sucrose
551 acceptance behavior in *Drosophila*. *Neuron*. 2012;73:941–50.
- 552 26. Zhou Y, Cao LH, Sui XW, Guo XQ, Luo DG. Mechanosensory circuits
553 coordinate two opposing motor actions in *Drosophila* feeding. *Sci Adv*.
554 2019;5:1–14.
- 555 27. Urban E, Nagarkar-Jaiswal S, Lehner CF, Heidmann SK. The Cohesin
556 Subunit Rad21 Is Required for Synaptonemal Complex Maintenance, but Not
557 Sister Chromatid Cohesion, during *Drosophila* Female Meiosis. Hawley RS,
558 editor. *PLoS Genet*. 2014;10:e1004540.
- 559 28. Caussin E, Kanca O, Affolter M. Fluorescent fusion protein knockout
560 mediated by anti-GFP nanobody. *Nat Struct Mol Biol*. 2012;19:117–21.
- 561 29. Lv P, Sheng Y, Zhao Z, Zhao W, Gu L, Xu T, et al. Targeted disruption of
562 *Rab10* causes early embryonic lethality. *Protein Cell*. 2015;6:463–7.
- 563 30. Harnois C, Di Paolo T. Decreased dopamine in the retinas of patients with
564 Parkinson's disease. *Invest ophthalmol vis sci*. 1990;31:2473.

- 565 31. Ortuño-Lizarán I, Sánchez-Sáez X, Lax P, Serrano GE, Beach TG, Adler CH,
566 et al. Dopaminergic retinal cell loss and visual dysfunction in Parkinson's
567 disease. *Ann Neurol.* 2020;
- 568 32. Franceschini N, Kirschfeld K. Les phénomènes de pseudopupille dans
569 l'œil composé de *Drosophila*. *Kybernetik.* 1971;9:159–82.
- 570 33. Gupta H V., Zhang N, Driver-Dunckley E, Mehta SH, Beach TG, Adler CH.
571 Contrast Acuity With Different Colors in Parkinson's Disease. *Mov Disord*
572 *Clin Pract.* 2019;6:672–7.
- 573 34. Monti JM, Monti D. The involvement of dopamine in the modulation of
574 sleep and waking. *Sleep Med Rev.* 2007;11:113–33.
- 575 35. Sitaraman D, Aso Y, Rubin GM, Nitabach MN. Control of Sleep by
576 Dopaminergic Inputs to the *Drosophila* Mushroom Body. *Front Neural*
577 *Circuits.* 2015;9:73.
- 578 36. Dubowy C, Sehgal A. Circadian Rhythms and Sleep in *Drosophila*
579 *melanogaster*. *Genetics.* 2017;205:1373–97.
- 580 37. Helfrich-Förster C. Sleep in Insects. *Annu Rev Entomol.* 2018;63:69–86.
- 581 38. Hirsh J, Riemensperger T, Coulom H, Iche M, Coupar J, Birman S. Roles of
582 Dopamine in Circadian Rhythmicity and Extreme Light Sensitivity of
583 Circadian Entrainment. *Curr Biol.* 2010;20:209–14.
- 584 39. Shohamy D, Adcock RA. Dopamine and adaptive memory. *Trends Cogn*
585 *Sci.* 2010;14:464–72.
- 586 40. Cognigni P, Felsenberg J, Waddell S. Do the right thing: neural network
587 mechanisms of memory formation, expression and update in *Drosophila*.
588 *Curr Opin Neurobiol.* 2018;49:51–8.
- 589 41. Takemura S ya, Aso Y, Hige T, Wong A, Lu Z, Xu CS, et al. A connectome
590 of a learning and memory center in the adult *Drosophila* brain. *Elife.* 2017;6:1–
591 43.
- 592 42. Montague SA, Baker BS. Memory elicited by courtship conditioning

- 593 requires mushroom body neuronal subsets similar to those utilized in
594 appetitive memory. *PLoS One*. 2016;11:1–24.
- 595 43. Eguchi T, Kuwahara T, Sakurai M, Komori T, Fujimoto T, Ito G, et al.
596 LRRK2 and its substrate Rab GTPases are sequentially targeted onto stressed
597 lysosomes and maintain their homeostasis. *Proc Natl Acad Sci*.
598 2018;115:E9115–24.
- 599 44. Rivero-ríos P, Romo-lozano M, Fernández B, Fdez E. Distinct roles for
600 RAB10 and RAB29 in pathogenic LRRK2-mediated endolysosomal trafficking
601 alterations. *Cells*. 2020;9.
- 602 45. Liu Z, Xu E, Zhao HT, Cole T, West AB. LRRK2 and Rab10 Coordinate
603 Macropinocytosis to Mediate Immunological Responses in Phagocytes. *EMBO*
604 *J*. 2020;e104862:1–21.
- 605 46. Dhekne HS, Yanatori I, Gomez RC, Tonelli F, Diez F, Schüle B, et al. A
606 pathway for Parkinson’s Disease LRRK2 kinase to block primary cilia and
607 Sonic hedgehog signaling in the brain. *Elife*. 2018;7:1–26.
- 608 47. Ordóñez AJL, Fernández B, Fdez E, Romo-Lozano M, Madero-Pérez J,
609 Lobbestael E, et al. RAB8, RAB10 and RILPL1 contribute to both LRRK2
610 kinase-mediated centrosomal cohesion and ciliogenesis deficits. *Hum Mol*
611 *Genet*. 2019;
- 612 48. Wauters F, Cornelissen T, Imberechts D, Martin S, Koentjoro B, Sue C, et al.
613 LRRK2 mutations impair depolarization-induced mitophagy through
614 inhibition of mitochondrial accumulation of RAB10. *Autophagy*. 2019;16:203–
615 22.
- 616 49. Beilina A, Bonet-Ponce L, Kumaran R, Kordich JJ, Ishida M, Mamais A, et
617 al. The Parkinson’s Disease Protein LRRK2 Interacts with the GARP Complex
618 to Promote Retrograde Transport to the trans-Golgi Network. *Cell Rep*.
619 2020;31.
- 620 50. Nakamura Y, Ochi Y, Satoh T, Satoh AK. Crag/Rab10/Ehbp1 regulate the
621 basolateral transport of Na + K + ATPase in *Drosophila* photoreceptors. *J Cell*

- 622 Sci. 2020;133:jcs.238790.
- 623 51. Lin C-H, Li H, Lee Y-N, Cheng Y-J, Wu R-M, Chien C-T. Lrrk regulates the
624 dynamic profile of dendritic Golgi outposts through the golgin Lava lamp. J
625 Cell Biol. 2015;210:471–83.
- 626 52. Kuwahara T, Inoue K, D'Agati VD, Fujimoto T, Eguchi T, Saha S, et al.
627 LRRK2 and RAB7L1 coordinately regulate axonal morphology and lysosome
628 integrity in diverse cellular contexts. Sci Rep. 2016;6:29945.
- 629 53. Schapansky J, Khasnavis S, DeAndrade MP, Nardoizzi JD, Falkson SR,
630 Boyd JD, et al. Familial knockin mutation of LRRK2 causes lysosomal
631 dysfunction and accumulation of endogenous insoluble α -synuclein in
632 neurons. Neurobiol Dis. 2018;111:26–35.
- 633 54. Rivero-Ríos P, Romo-Lozano M, Fasiczka R, Naaldijk Y, Hilfiker S.
634 LRRK2-Related Parkinson's Disease Due to Altered Endolysosomal Biology
635 With Variable Lewy Body Pathology: A Hypothesis. Front Neurosci.
636 2020;14:1–16.
- 637 55. Driscoll M, Coleman V, McLaughlin M, Nguyen A, Sitaraman D.
638 Dopamine neurons promote arousal and wakefulness via Dop1R receptor in
639 the *Drosophila* mushroom body. bioRxiv. 2020;2020.04.29.069229.
- 640 56. Potdar S, Sheeba V. Wakefulness Is Promoted during Day Time by PDFR
641 Signalling to Dopaminergic Neurons in *Drosophila melanogaster*. eNeuro.
642 2018;5:ENEURO.0129-18.2018.
- 643 57. Soukup SF, Kuenen S, Vanhauwaert R, Manetsberger J, Hernández-Díaz S,
644 Swerts J, et al. A LRRK2-Dependent EndophilinA Phosphoswitch Is Critical
645 for Macroautophagy at Presynaptic Terminals. Neuron. 2016;92:829–44.
- 646
- 647

648 **Figure legends**

649 **Fig. 1. Validation of Rab10 depletion and phosphorylation *in vivo*.** A. A
650 pan-hRab10 antibody detects dRab10 and shows that Rab10 is increased by
651 neuronal (nSyb-GAL4) expression of UAS-*Rab10*, abolished in the Rab10⁻
652 null, and substantially reduced by neuronal expression of *Rab10^{RNAi}*.
653 Antibody-specificity was confirmed by rat CNS binding. B. A phospho-
654 hRab10 antibody detects phospho-dRab10, which is increased by neuronal
655 expression of UAS-*Rab10*, but undetectable with the Rab10⁻ null or with
656 neuronal expression of *Rab10^{RNAi}*. C. Validation of deGradFP technique. In
657 flies where endogenous *Rab10* has been replaced by *YFP-Rab10*, global (Act5c-
658 GAL4) or neuronal expression of the vhhGFP nanobody reduces the level of
659 YFP-Rab10 by ~50%. A slightly smaller reduction is achieved by neuronal
660 expression of *GFP^{RNAi}*. D. Neuronal expression of *Rab10* increases pRab10, as
661 does neuronal expression of *LRRK2-G2019S*. Neuronal expression of a kinase-
662 dead *LRRK2* (*KD*, *LRRK2-G2019S-K1906M*) has no effect on the
663 phosphorylation of Rab10. B. Quantification of the Western blots in the
664 corresponding panels of A. Loading control: α -drosophila-synaptotagmin (α -
665 syt). Exact genotypes and in Table S2.

666 **Fig. 2. *Rab10* knock-down rescues *LRRK2-G2019S* -induced bradykinesia.**
667 **A. Optogenetic stimulation of the Proboscis Extension Response (PER).** Ai.
668 To reach for food or liquid, the fly extends its proboscis in response to an
669 optogenetic stimulus to sensory neurons on the legs. The full extension
670 response is shown in Movie M1. Aii Expression of *LRRK2-G2019S* in
671 dopaminergic neurons (*THG2*) reduces the proportion of flies that respond to
672 a single flash of light, and this is rescued by Rab10 reduction with *Rab10^{RNAi}*.
673 Aiii. Dopaminergic reduction in Rab10 rescues the bradykinesia (slower
674 response) of flies expressing *G2019S* in their dopaminergic neurons. Aiii. Raw
675 traces; Aiv. mean data. To respond to the optogenetic stimuli all flies carry
676 *LexA/Op Gr5a>ReachR*. **B. Sucrose stimulation of the PER.** Bi. Flies expressing
677 *G2019S* in their dopaminergic neurons (*THG2*, magenta bars) respond less
678 frequently to sucrose than wild-type flies (green) i.e. they show akinesia. This

679 is rescued in *THG2* flies with dopaminergic reduction in Rab10 using
680 *Rab10^{RNAi}* (*THG2 > Rab10^{RNAi}*). Bii Reduction of dopaminergic Rab10 with the
681 deGradFP technique (*Rab10 GFP; THG2>vhhGFP*, yellow bars) also rescues
682 the *G2019S*-induced akinesia. Biii. The Rab10 null (*Rab10⁻*, orange bar) also
683 reverts the *G2019S* deficit, while expression of *Rab10* in the null background
684 again induces akinesia (*Rab10⁻; TH > Rab10*, light blue bar). Biv. By itself,
685 *Rab10* expression phenocopies *THG2*. Exact genotypes and full statistical data
686 in Table S3.

687 **Fig. 3. Visual degeneration due to *LRRK2-G2019S* is rescued by**
688 **dopaminergic knock-down of *Rab10*. A. Anatomically, dopaminergic *Rab10***
689 **knock-down rescues the loss of eye structure.** Ai. Healthy flies have a
690 marked DPP (Deep-Pseudo-Pupil) which can be seen when the eye is
691 illuminated from underneath. Light passing directly through the eye is focused
692 towards the observer, but light at an angle is blocked by the pigmentation in
693 the ommatidia. Aii-Aiv. PD-mimic flies (*THG2; vhhGFP*) kept in the dark for
694 14 days lose their focused DPP as the eyes show an increased number of
695 ommatidia transmitting light, spread over a wider area, with the loss of
696 pigmentation indicating lysosomal dysfunction. Much less degeneration is
697 seen when Rab10 is depleted using the deGradFP technique (*YFP-Rab10;*
698 *THG2; vhhGFP* flies). B. **Physiologically, dopaminergic *Rab10* knock-down**
699 **rescues neuronal vision.** Bi. Degeneration is accelerated by a mild visual
700 stress achieved by keeping the flies in ‘disco-chambers’ where the light is
701 turned on and off approximately every 2 seconds; these flies were compared
702 with those kept in the dark. Bii-iii. Flies kept in the dark have normal visual
703 responses after 7 days. However, *THG2* flies in disco chambers lose their
704 physiological response after 7 days (hatched magenta bar, controls in green).
705 This is rescued by deGradFP mediated knockdown of Rab10 protein (Bi,
706 *Rab10 GFP; THG2; vhhGFP* hatched yellow bar) or by dopaminergic knock-
707 down of Rab10 by *RNAi* (Bii, *THG2 > Rab10RNAi* yellow bar). Exact
708 genotypes and statistical data in Table S3.

709 **Fig 4. *Rab10* knock-down does not rescue sleep deficits induced by**
710 **dopaminergic expression of *LRRK2-G2019S*.** A. There is no effect of *LRRK2-*
711 *G2019S* or *Rab10* expression on circadian period in continuous darkness (DD),
712 and only a small reduction in circadian period when both genes are
713 expressed. Ai. Raw actograms; Aii mean period from days 6-9 in DD. B. In
714 Light/dark (LD), *THG2* flies show increased sleep during the day, and
715 reduced sleep at night. Neither reduced nor increased expression of *Rab10*
716 affects the daily pattern of sleep (Bi), with summary data in Bii. Sleep is
717 defined as periods of inactivity longer than 5 min. Exact genotypes and
718 statistical results in Table S5.

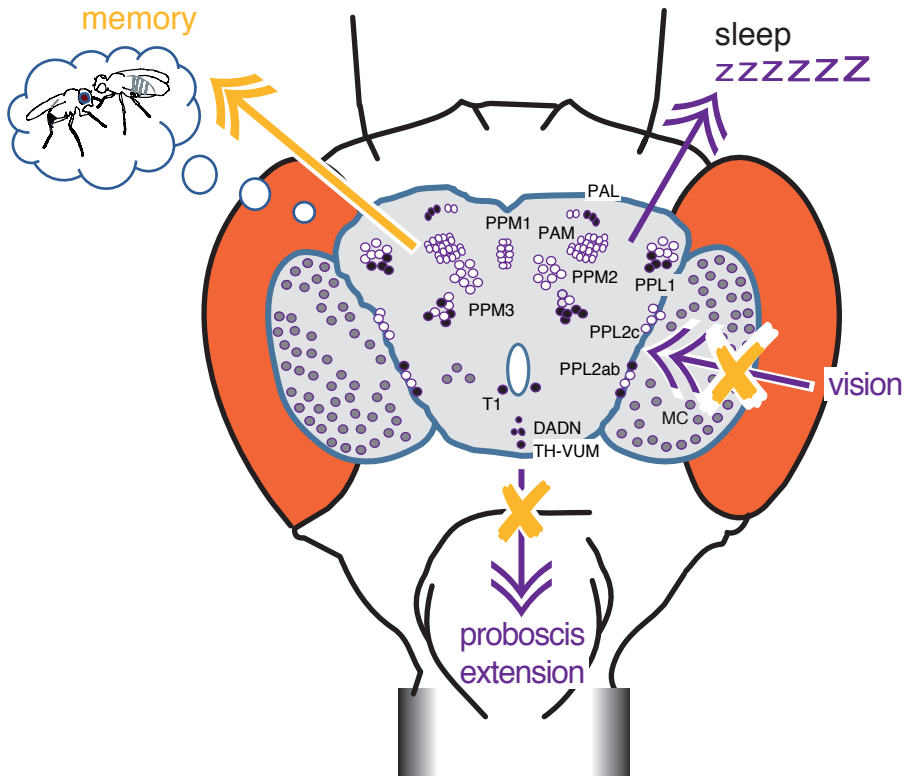
719 **Fig. 5. Memory depends on dopaminergic *Rab10* but not *LRRK2-G2019S*.** A.
720 Depletion of *Rab10* in the control background (*TH > Rab10^{RNAi}*) increases the
721 proportion of flies with low memory index (MI) compared to flies with no
722 transgene expression (*TH/+*). B. Expression of *LRRK2-G2019S* has no effect on
723 performance; either for the *THG2/+ v TH/+* control flies, nor for the flies with
724 *Rab10^{RNAi}*. Exact genotypes and statistical results in Table S6.

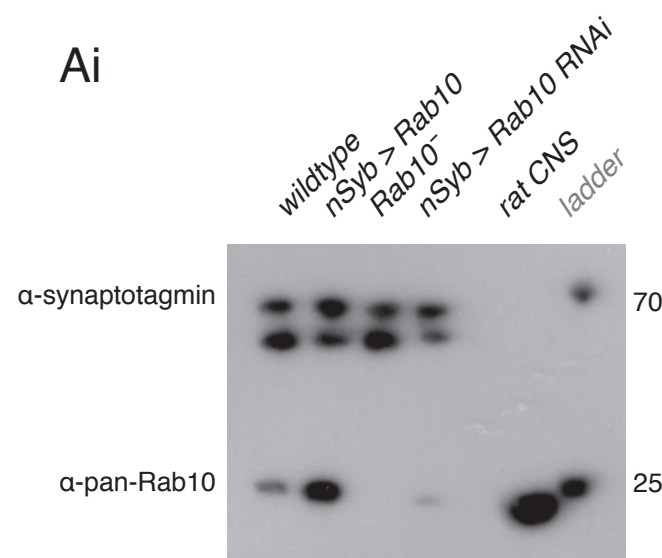
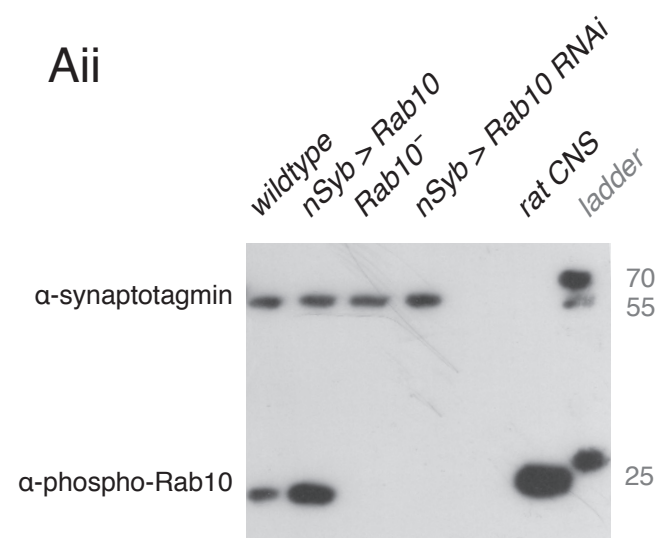
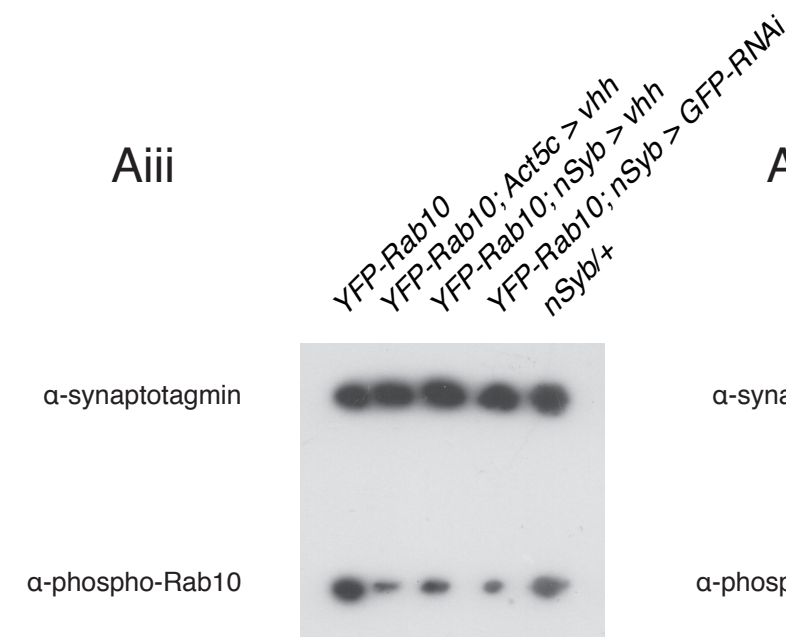
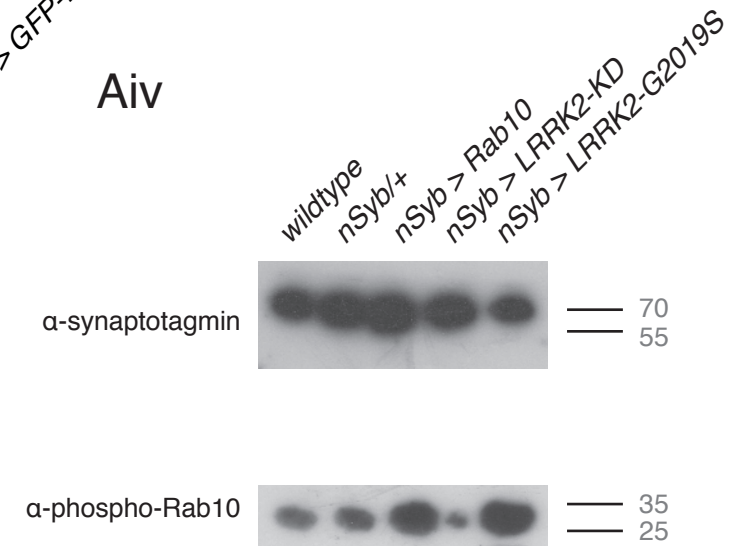
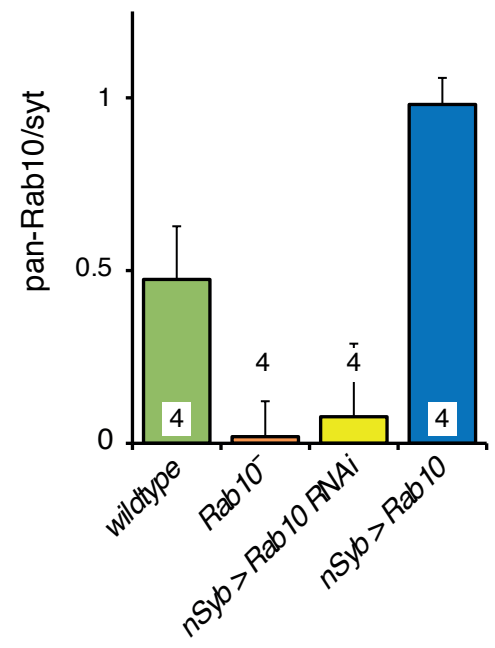
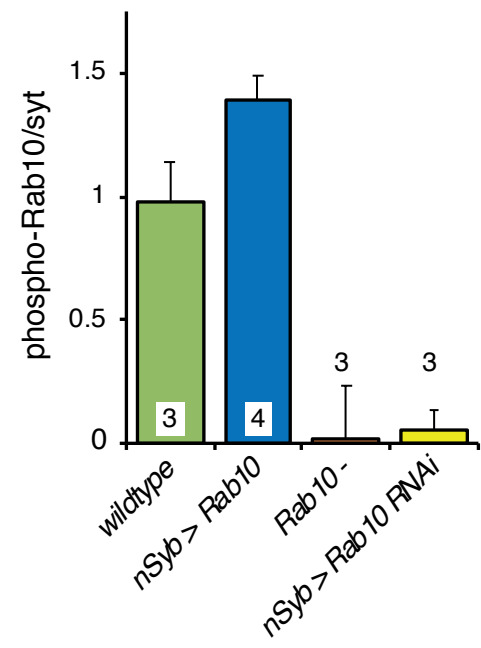
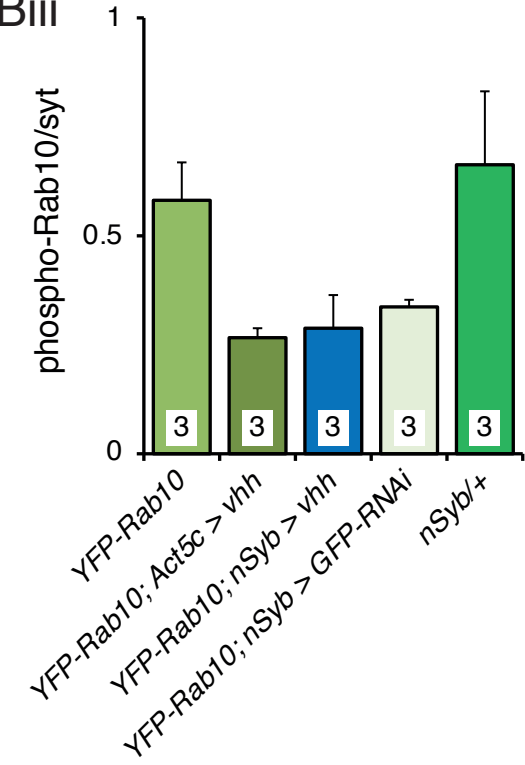
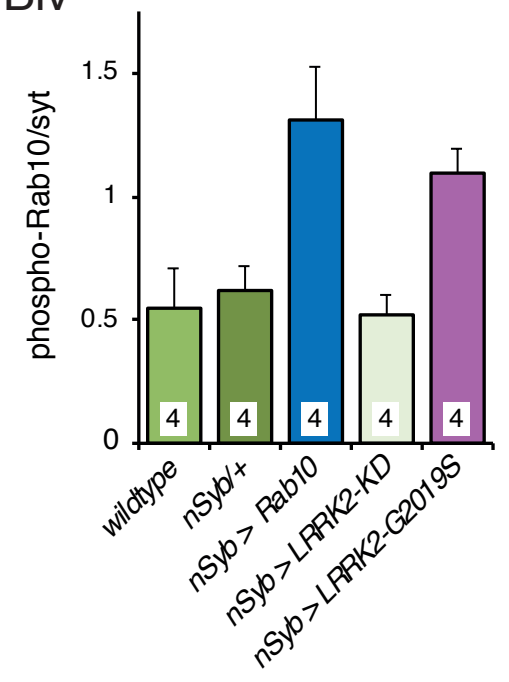
725 **Fig. 6. *LRRK2-G2019S* is found in the cytoplasm of the cell soma and in the**
726 **synaptic endings of dopaminergic neurons.** A. Confocal stack through the
727 TH-VUM and DADN neurons in the ventral part of the brain of a *THG2 >*
728 *mCD8-GFP* fly. Note that *LRRK2* protein is found more in the cytoplasm than
729 the nucleus, and that there are areas of the cytoplasm with less *LRRK2*
730 staining. *mCD8-GFP* expression is used to mark dopaminergic neurons. B.
731 Dopaminergically expressed *Rab10-YFP* is found in the synaptic endings in
732 the mushroom bodies (MB) and weakly in the fan-shaped body (FB). Stack of
733 two confocal images. C. *THG2* flies show *LRRK2* protein in the dopaminergic
734 cell bodies (PPL, THV, DADN) and in the synaptic neuropil, of the mushroom
735 bodies. Single confocal section with α -*LRRK2* antibody. Images representative
736 of at least 3 preparations. Exact genotypes in Table S7.

737 **Movie M1. Extension of the proboscis in response to an optogenetic**
738 **stimulus.** A flash of blue light is used to excite the *GR5a* sugar-sensitive

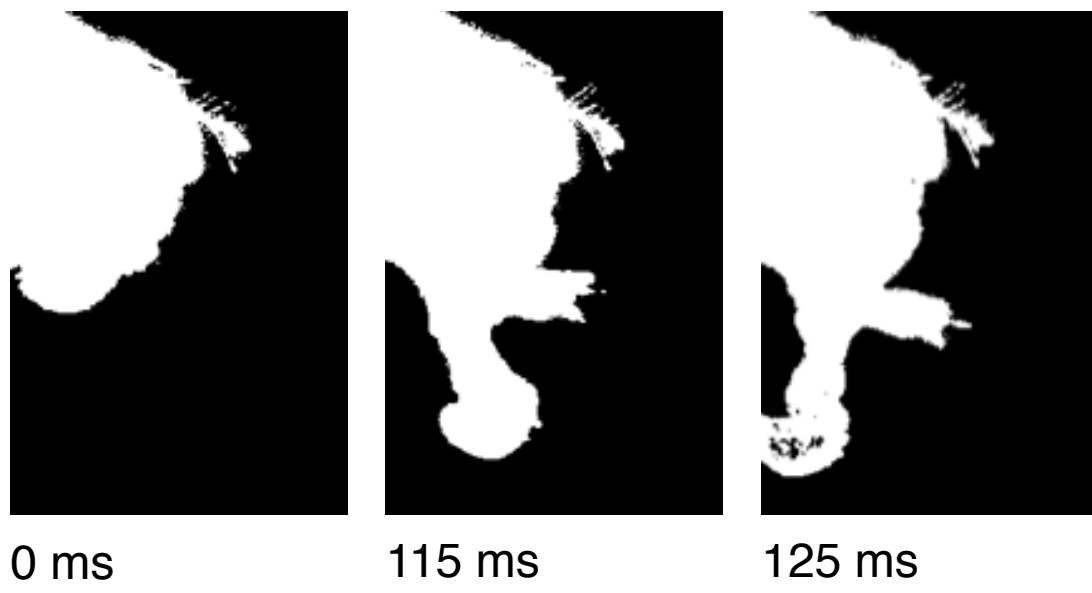
739 neurons which leads to the extension of the proboscis. The outline of the fly
740 (red line) was determined by thresholding. The distance between the fixed
741 reference point and the lowest point of the proboscis (cyan dots) was
742 measured automatically on each frame. The recorded trace is shown as the
743 green line in Fig. 2Aiii. Each frame is 6 ms. Exact genotype: *Gr5a::ReachR* / + ;
744 +/+.

745

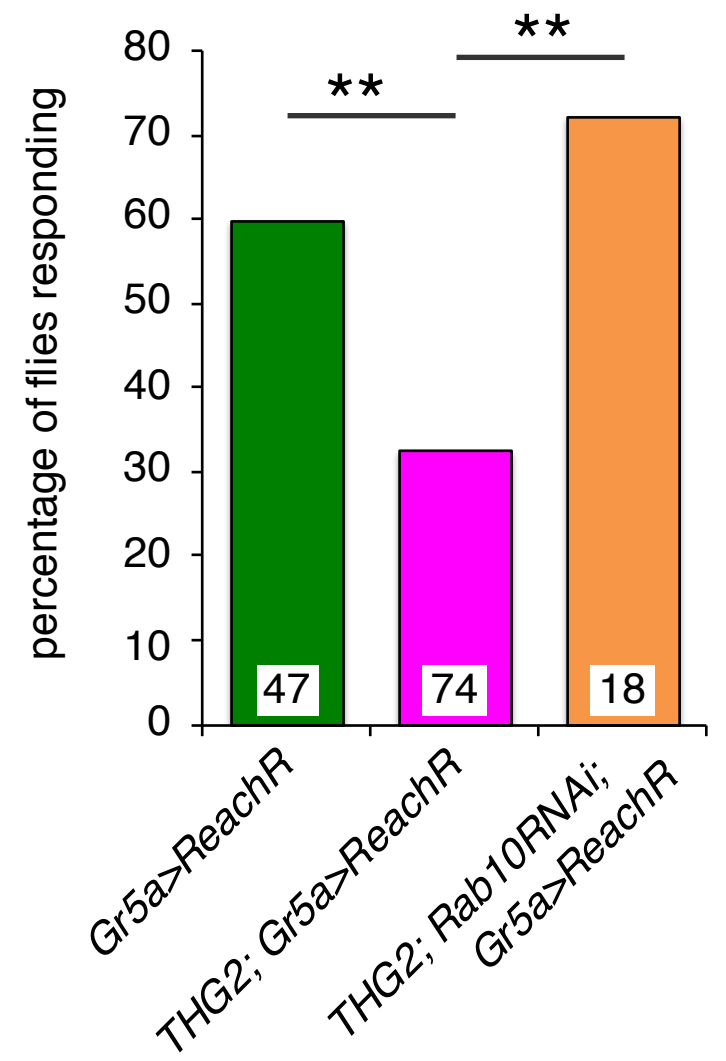


Ai**Aii****Aiii****Aiv****Bi****Bii****Biii****Biv**

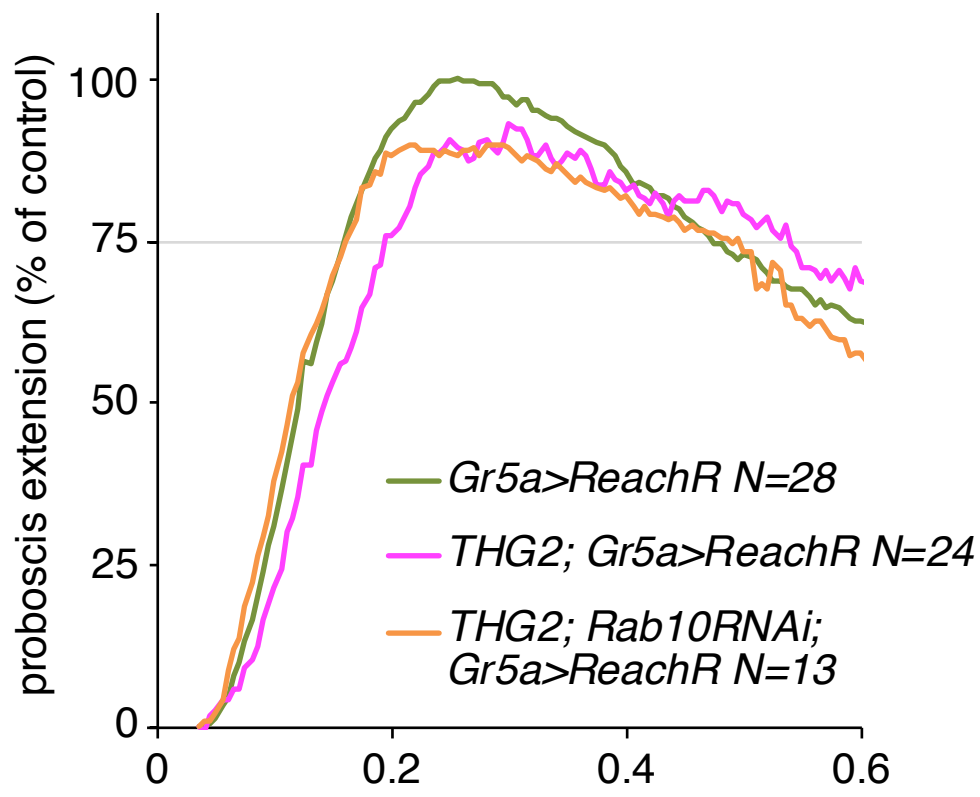
A Optogenetic (LexA/LexOp) (i)



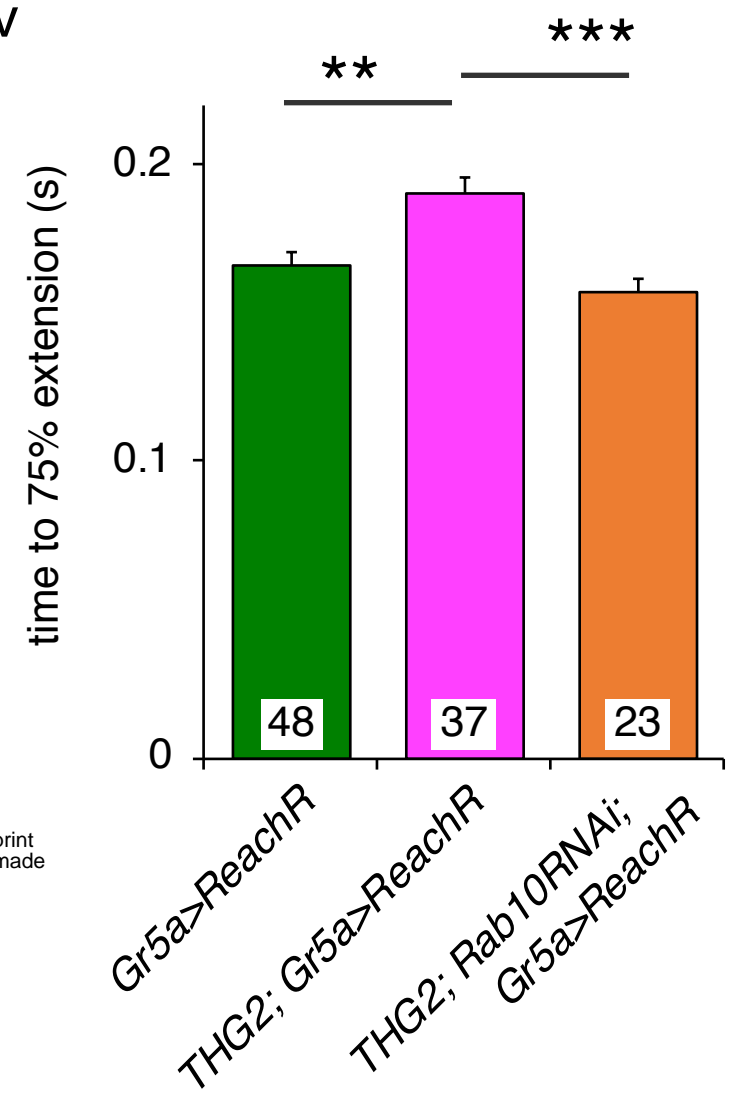
Aii



Aiii

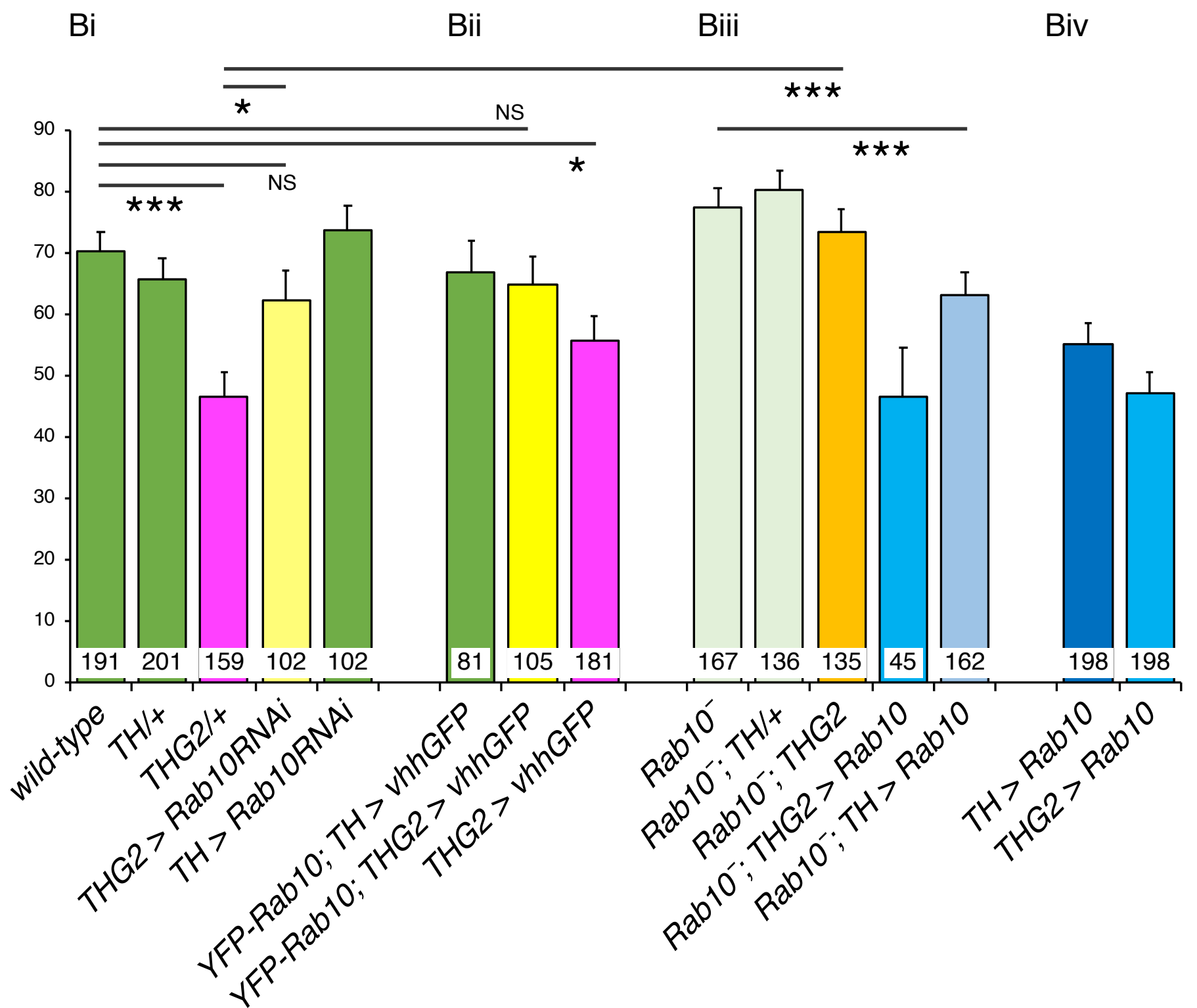


Aiv



bioRxiv preprint doi: <https://doi.org/10.1101/2020.09.28.316992>; this version posted October 12, 2020. The copyright holder for this preprint (which was not certified by peer review) is the author/funder, who has granted bioRxiv a license to display the preprint in perpetuity. It is made available under aCC-BY 4.0 International license.

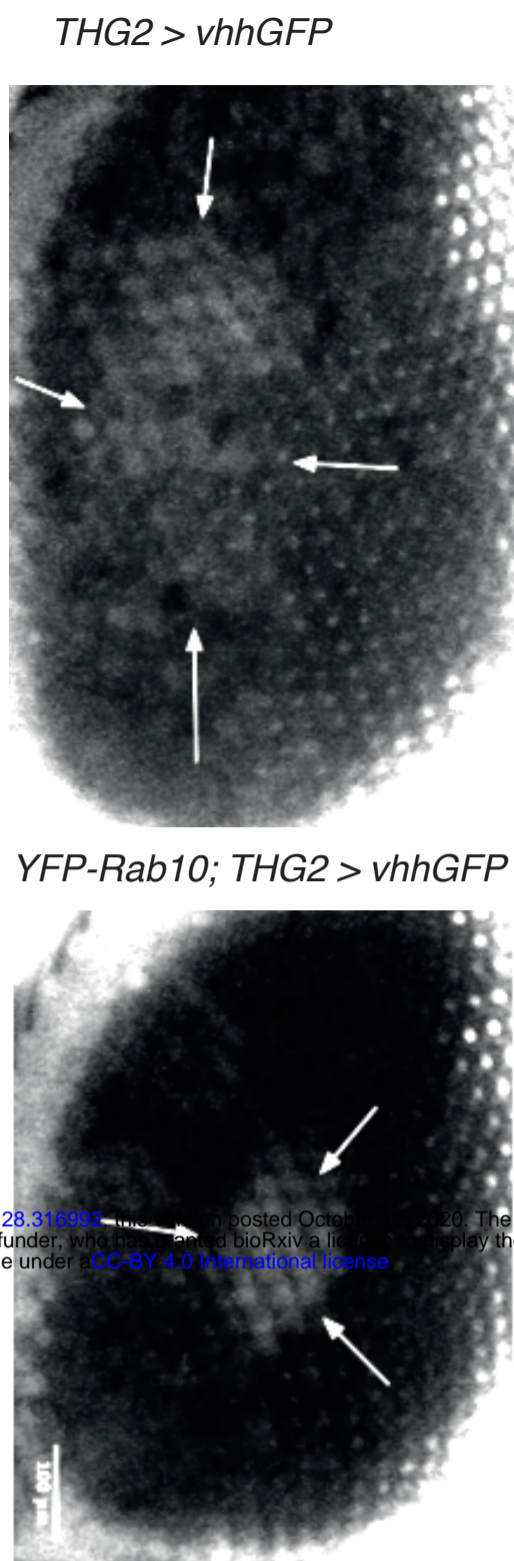
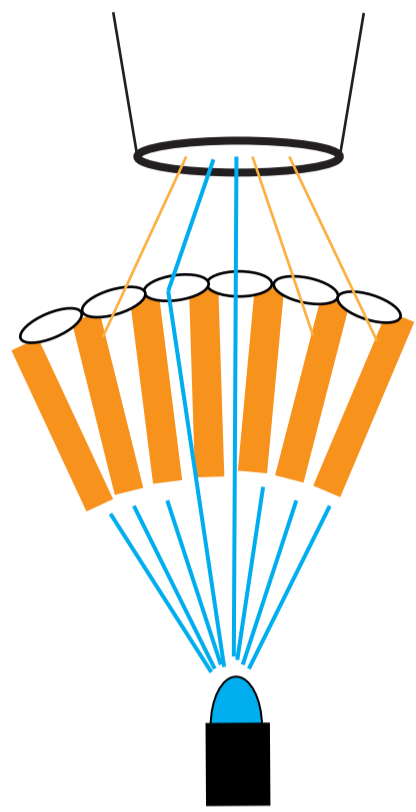
B sucrose



A Anatomical degeneration

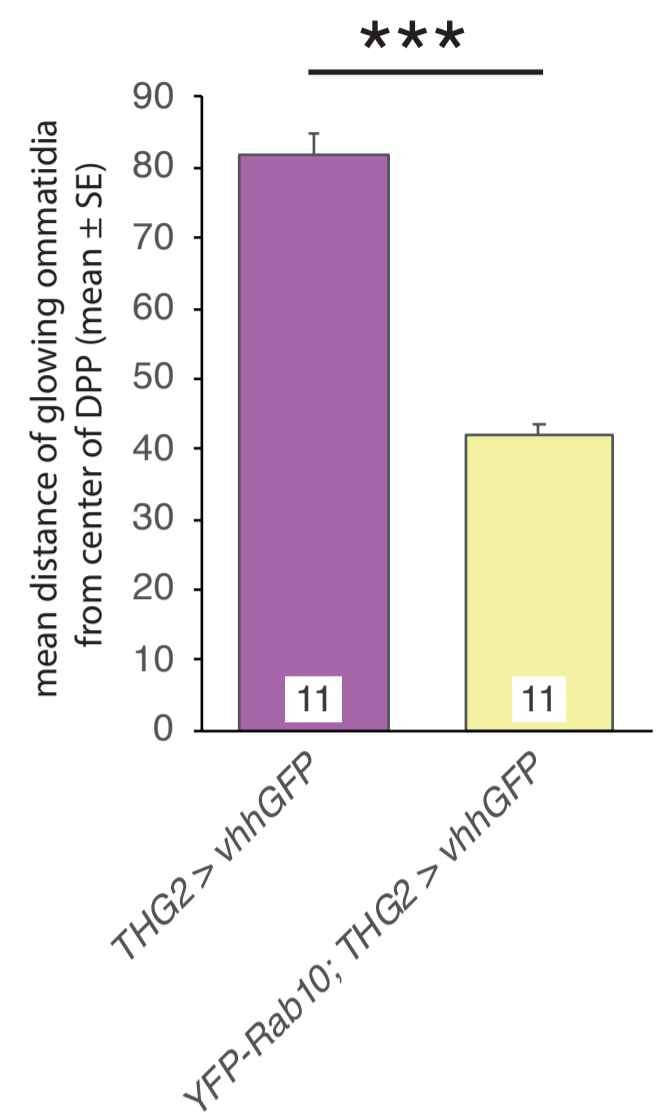
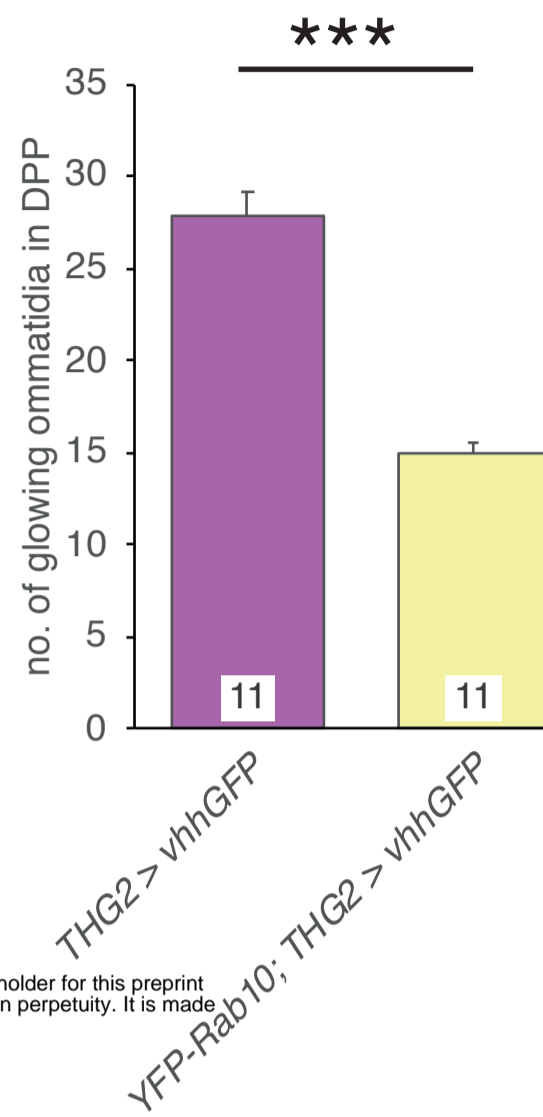
Ai

Aii



Aiii

Aiv



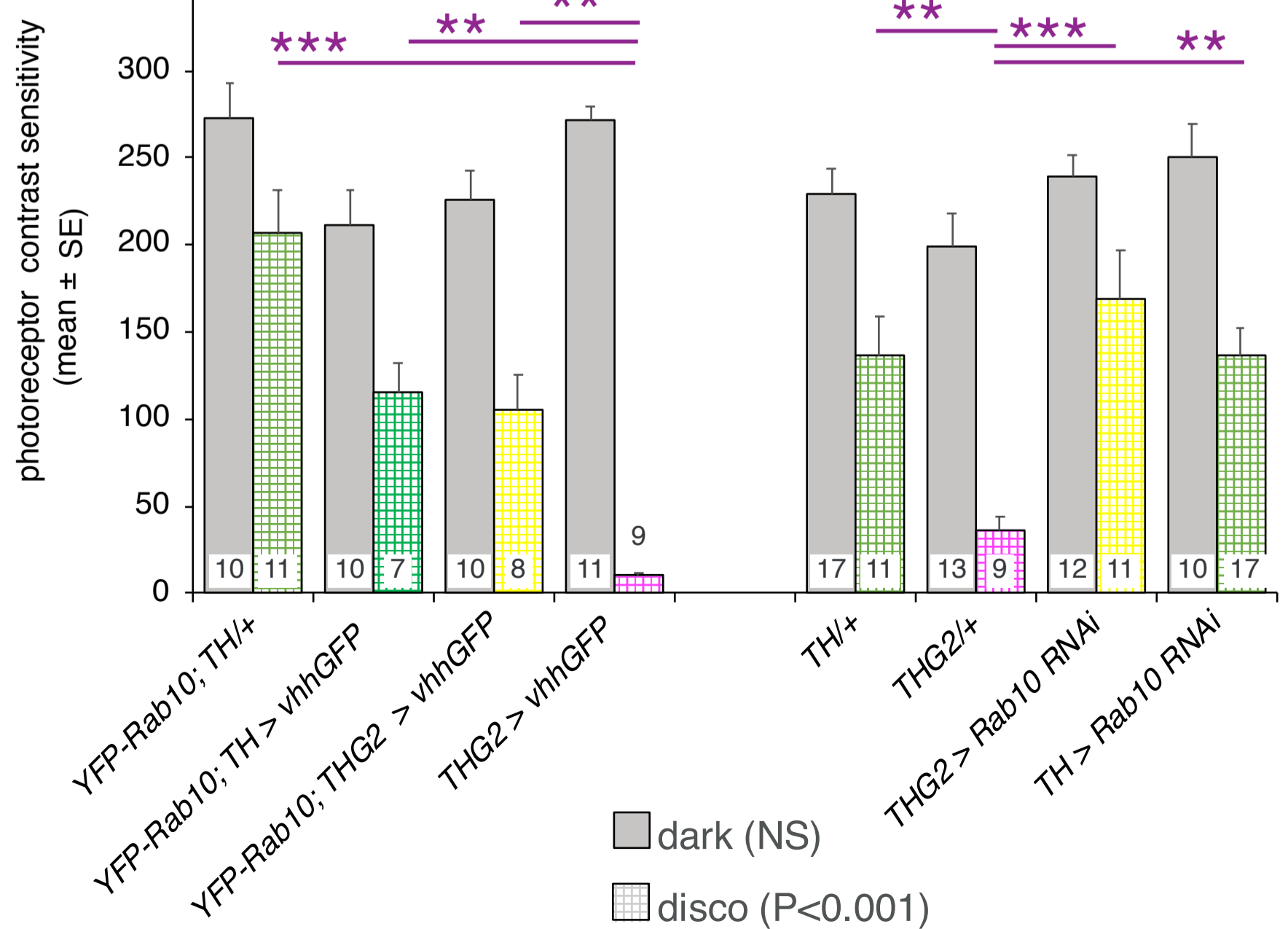
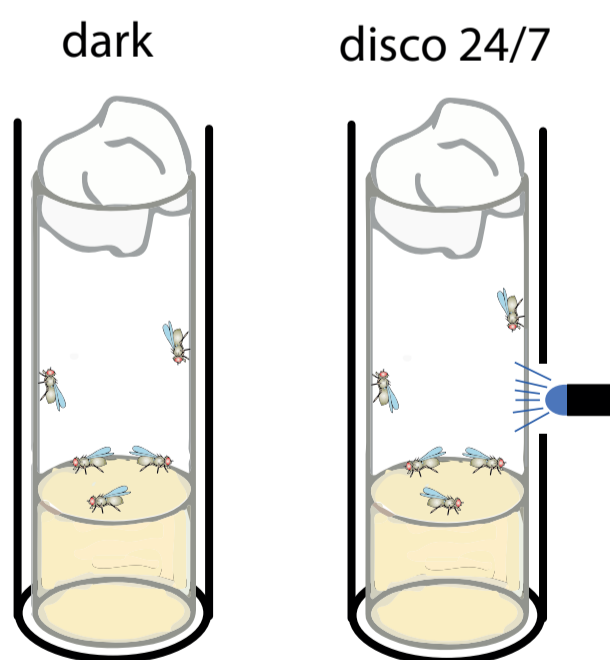
bioRxiv preprint doi: <https://doi.org/10.1101/2020.09.28.316092>; this version posted October 1, 2020. The copyright holder for this preprint (which was not certified by peer review) is the author/funder, who has granted bioRxiv a license to display the preprint in perpetuity. It is made available under aCC-BY 4.0 International license.

B Physiological degeneration

Bi

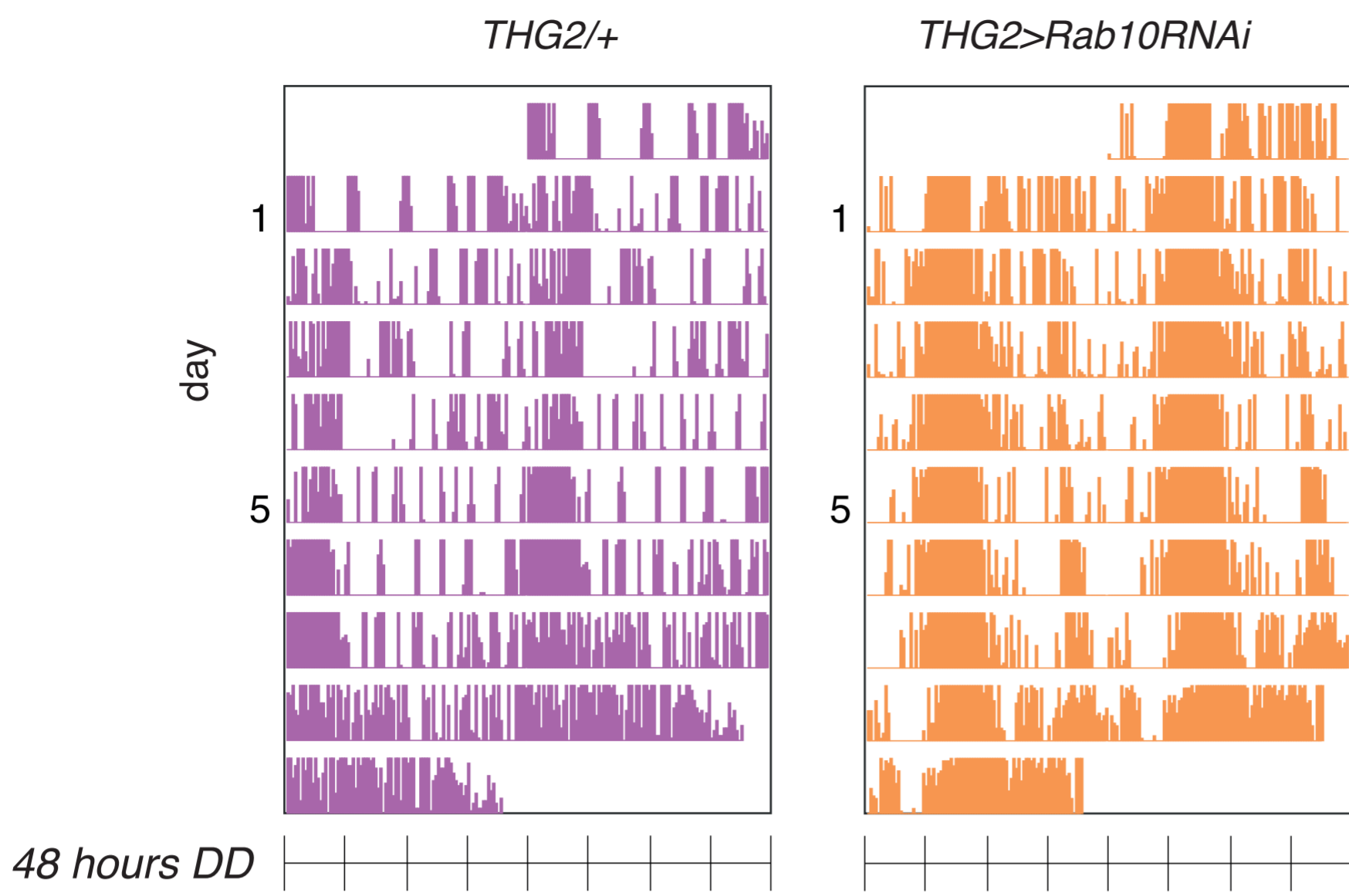
Bii

Biii

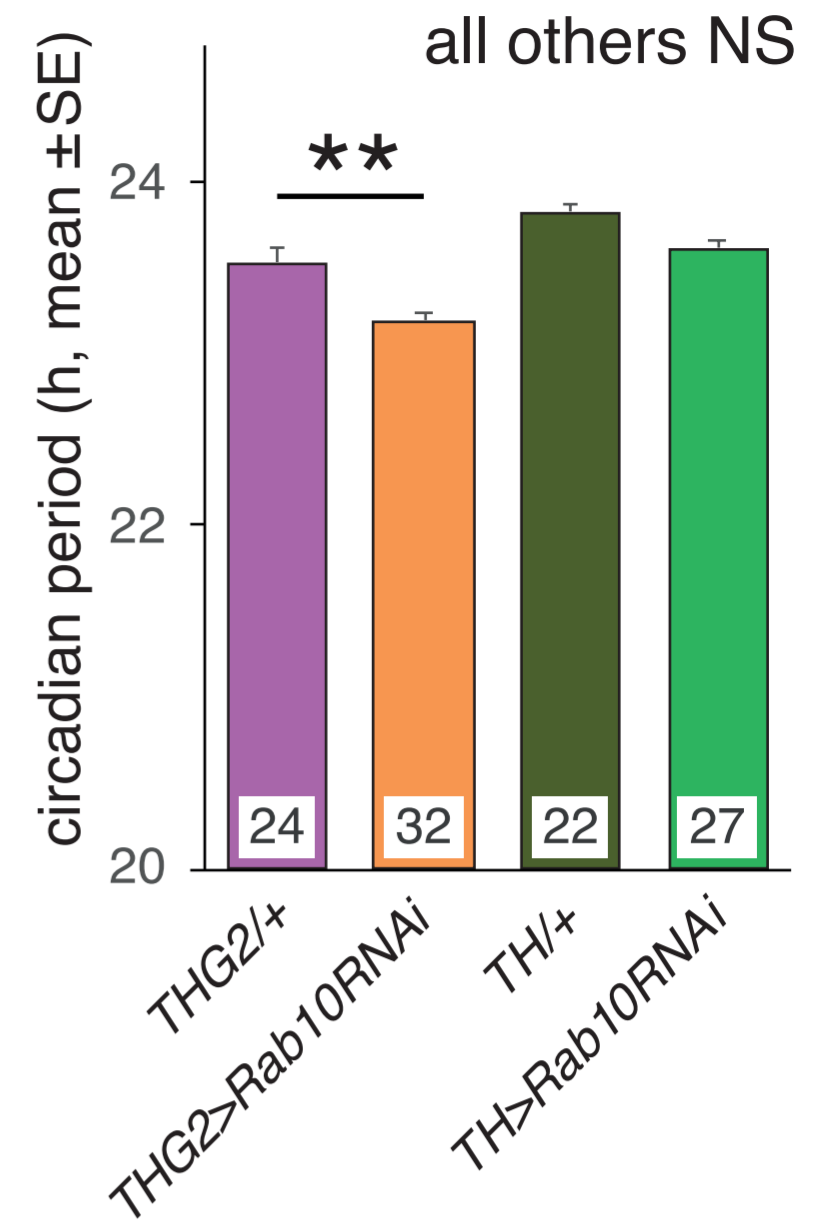


A: DD

Ai

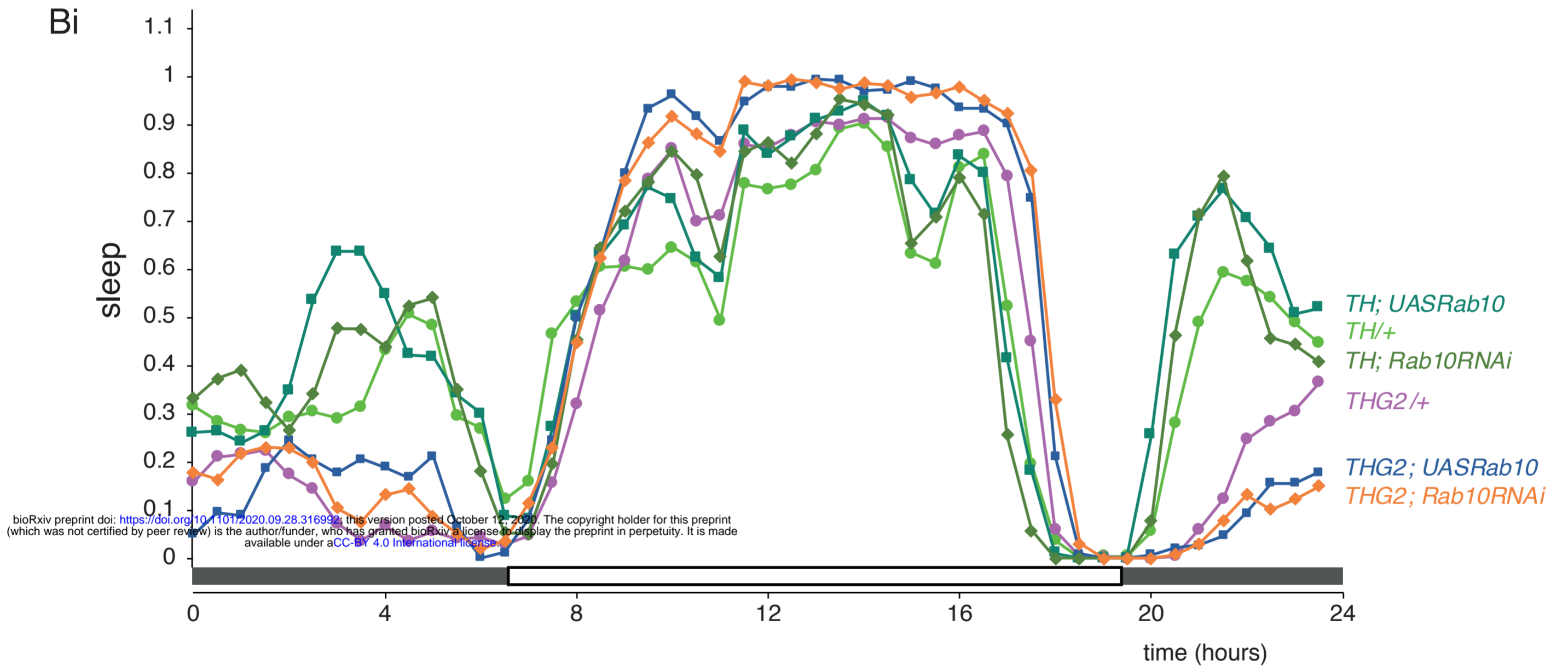


Aii

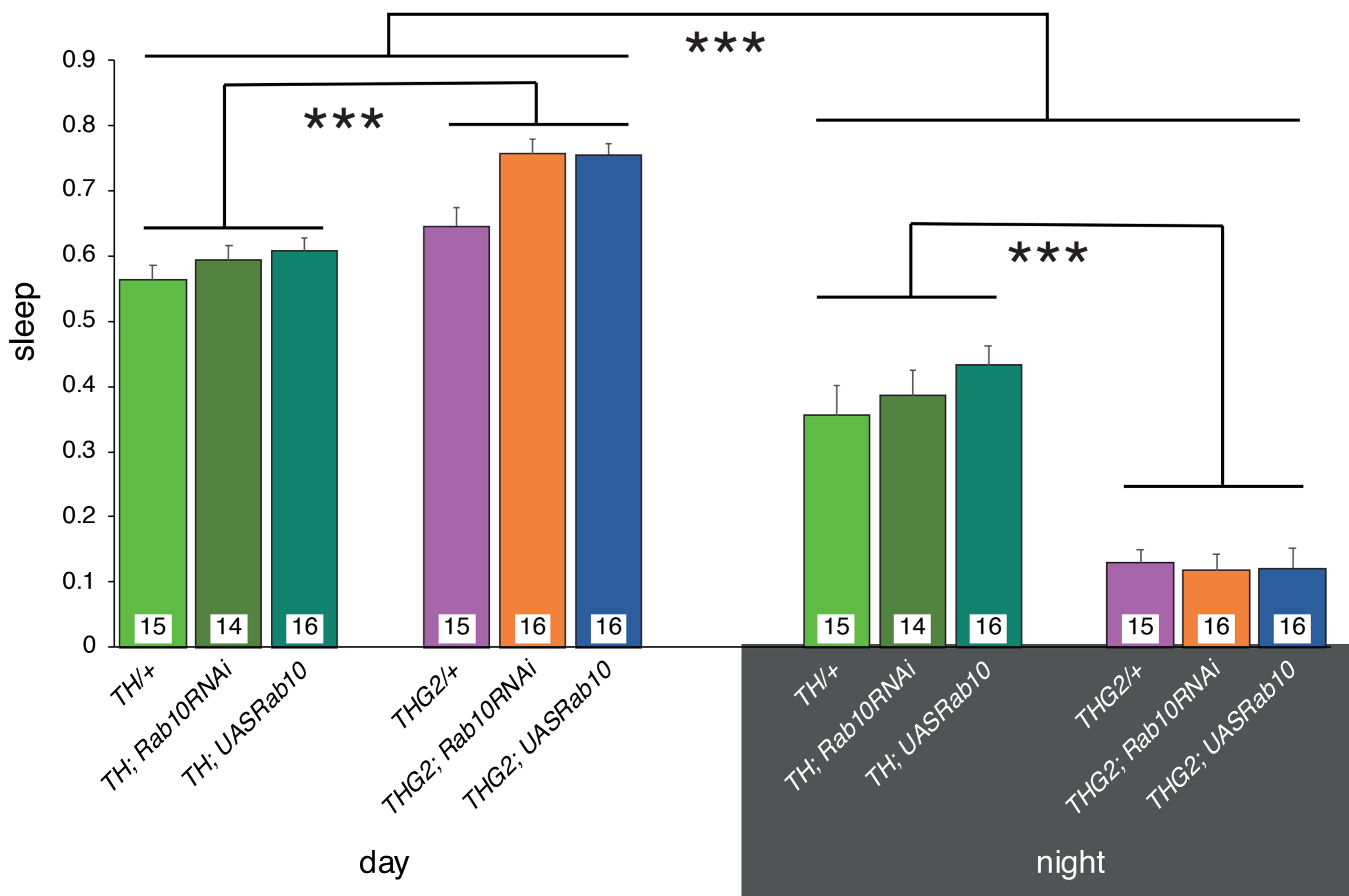


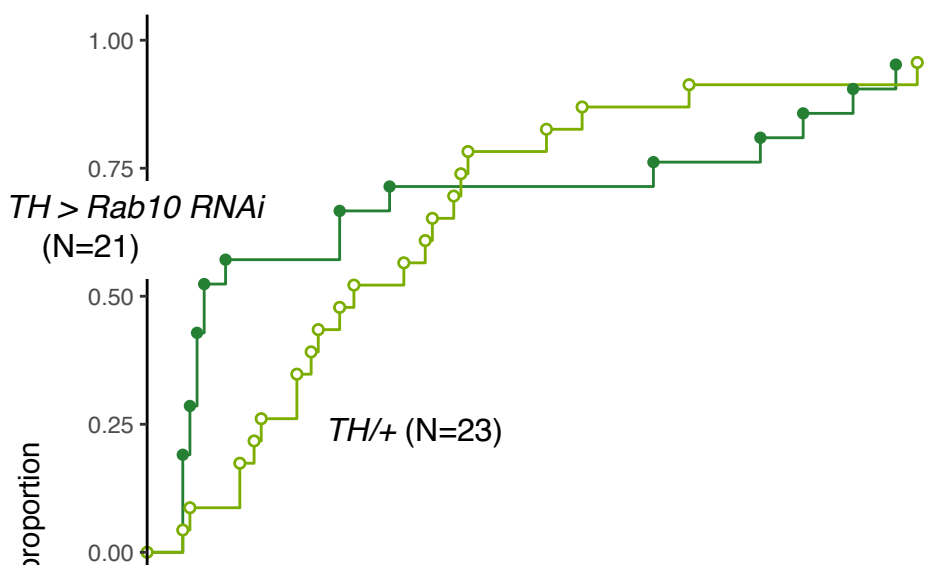
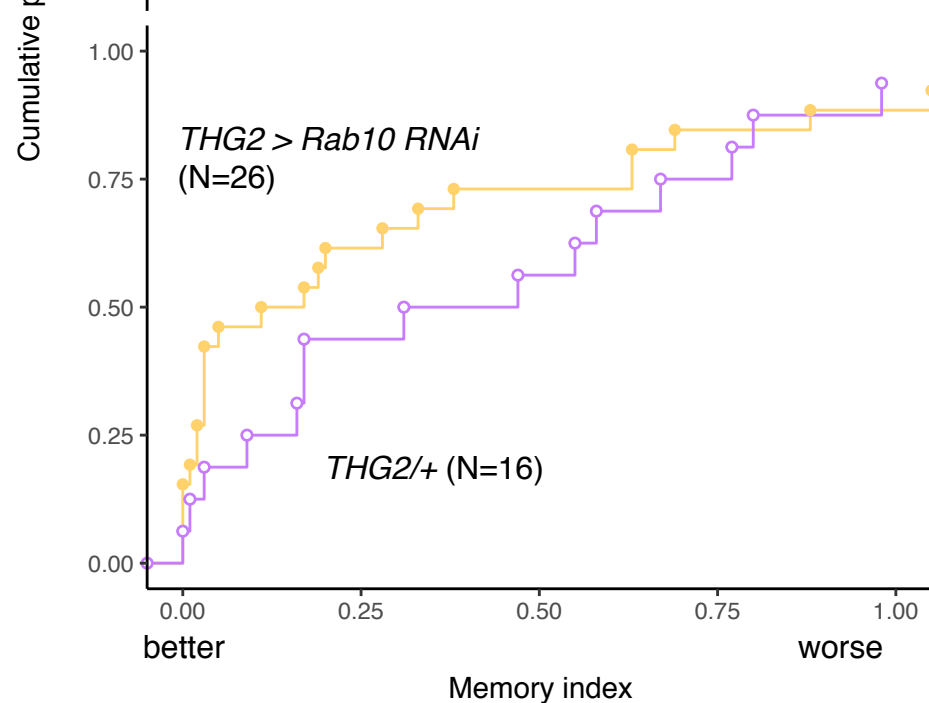
B : LD

Bi



Bii



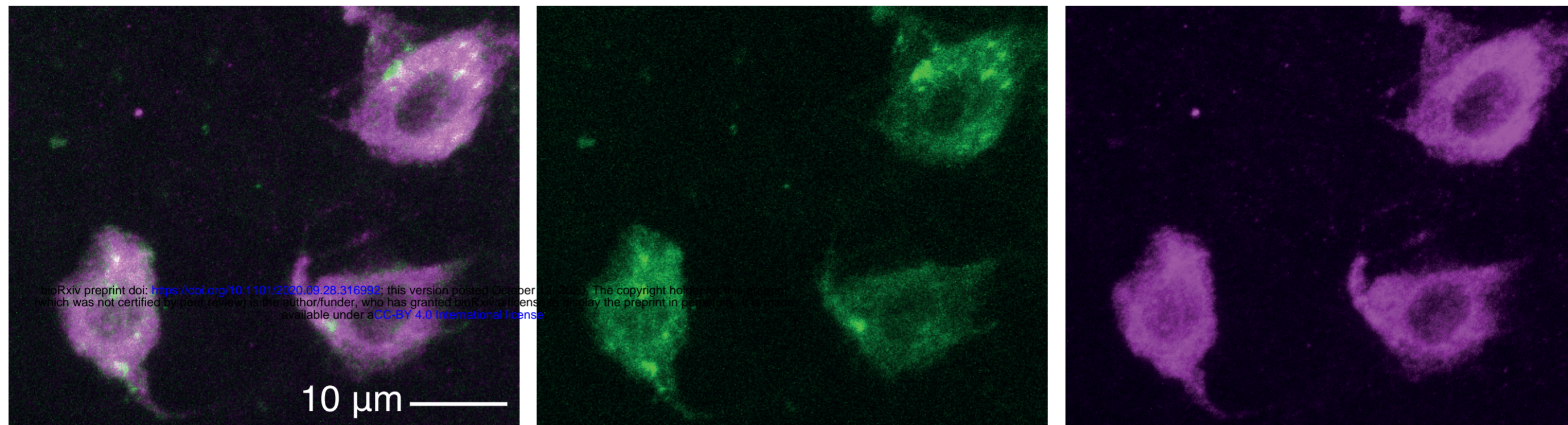
A**B**

A *THG2 > mCD8-GFP*

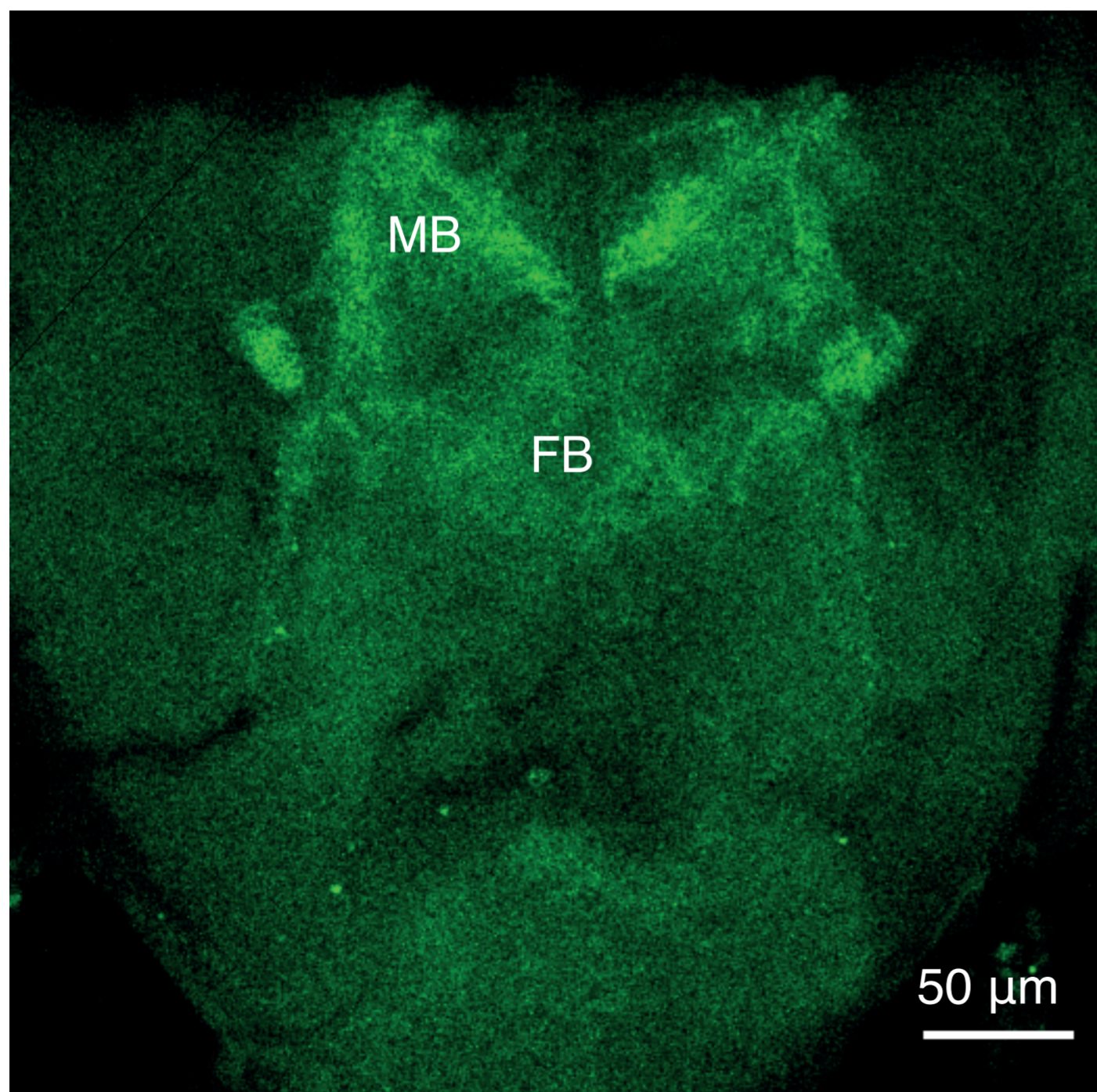
GFP/ α -LRRK2

GFP

α -LRRK2



B *TH > Rab10-YFP*



C *THG2* α -LRRK2

